

# ***Tectonic geomorphology and the record of Quaternary plate boundary deformation in the Olympic Mountains***

**Frank J. Pazzaglia**

*Department of Earth and Environmental Sciences, Lehigh University, Bethlehem, Pennsylvania 18015, USA*

**Glenn D. Thackray**

*Department of Geosciences, Idaho State University, Pocatello, Idaho 83209, USA*

**Mark T. Brandon**

*Department of Geology and Geophysics, Yale University, New Haven, Connecticut 06520-8109, USA*

**Karl W. Wegmann**

*Washington Department of Natural Resources, Division of Geology & Earth Resources, Olympia, Washington 98504-7007, USA*

**John Gosse**

*Department of Earth Sciences, Room 3006, Life Sciences Centre, Dalhousie University, Halifax, Nova Scotia B3H 4J1, Canada*

**Eric McDonald**

*Desert Research Institute, Division of Earth and Ecosystem Sciences, 2215 Raggio Parkway, Reno, Nevada 89512, USA*

**Antonio F. Garcia**

*Department of Physics, California Polytechnic State University, San Luis Obispo, California 93407, USA*

**Don Prothero**

*Department of Geology, Occidental College, 1600 Campus Road, Los Angeles, California 90041-3314, USA*

## **ABSTRACT**

**We use Quaternary stratigraphy to reconstruct landscape evolution and measure tectonic deformation of the Olympic Mountains section of the Pacific Northwest Coast Range. An important motivation for understanding orogenesis here, and throughout the Coast Range, is the concern about the relationship of active deformation to seismic hazards associated with the Cascadia subduction zone. There is also much interest in apportioning the nature of the deformation, whether cyclic or permanent, whether it involves mainly shortening parallel or normal to the margin, and how the deformation on the pro- versus retrowedge sides of the orogen compare. Pre-Holocene stratigraphy and structure provide the only records of sufficient duration to separate long-term permanent deformation from earthquake-cycle elastic deformation. For this reason, active-tectonic studies have focused on deformation of Quaternary deposits and landforms, which are best preserved along the Pacific Coast and offshore on the continental shelf. At least four major glacial advances are recorded in the valley and coastal deposits along the western margin of the Olympic Peninsula. Both numeric and relative dating, including soils of these deposits, establish a stratigraphic anchor that is used to document the relationship between margin parallel and margin normal deformation in**

**the Olympic Mountains, which, on a geologic time scale ( $>10^3$  yr), seems to be the fastest deforming part of the Cascadia forearc high. The glacial stratigraphic framework is extended to fluvial terraces of the Clearwater drainage, which remained unglaciated during the late Pleistocene and Holocene, preserving a record of river incision, with each terrace recording the shape and height of past long profiles. We assess how fluvial terraces are formed in this tectonically active setting and then use features of the terraces to estimate incision rates along the Clearwater long profile. The long fluvial history preserved in the Clearwater ensures that the unsteady deformation associated with the earthquake cycle is averaged out, leaving us with a record of long-term rock uplift as well as horizontal shortening. We show, however, that the earthquake cycle may play an important role in terrace genesis at the millennial time scale.**

**Keywords:** geomorphology, active tectonics, subduction wedges, glacial geology, soils, terraces.

## INTRODUCTION

We designed a 4-day field trip to exhibit the geology, geomorphology, and active tectonics of the Olympic Peninsula. The trip is the culmination of over a decade of collaborative research in the Olympic Mountains by the authors and their colleagues. The following text and figures are culled from numerous published papers and theses that report the findings of this research, namely, Brandon and Vance (1992), Thackray (1996, 1998, 2001), Wegmann (1999), Brandon et al. (1998), Pazzaglia and Brandon (2001), Wegmann and Pazzaglia (2002), and Tomkin et al. (2003). It is organized around four major topics that should generate lively discourse on how to use and interpret basic field relationships in tectonic geomorphology research: (1) How are complexly juxtaposed glacial, fluvial, and eolian surficial deposits and their corresponding soils assembled into a dated stratigraphic framework in a tectonically active setting?; (2) What is a river terrace, how is it made, and what do river terraces tell us about active tectonics?; (3) What is driving orogenesis for the Olympic Mountain segment of the Cascadia subduction zone? Is it shortening parallel to the direction of plate convergence, shortening normal to the direction of plate convergence, or some combination of both? Are there any geomorphic or stratigraphic field relationships that can actually be used to track the horizontal movement of rocks and thus interpret the shortening history over geologic time scales? How do the tectonics on the prowedge versus the retrowedge sides of the Olympic Mountains compare?; (4) We know that uplift along Cascadia includes the effects of cyclic earthquake-related deformation and long-term steady deformation. How do these different types of uplift influence incision and aggradation in the rivers of the Olympic Mountains?

The trip begins by laying out the big-picture tectonic setting. The concept of a pro- and retrowedge is introduced and exhibited on the eastern flank and core of the range. Geologic and thermochronologic evidence for margin parallel versus margin normal shortening is introduced. We then begin building a Quaternary stratigraphic foundation anchored along the western coast of the Olympic Peninsula that will be extended landward into the Clearwater drainage. As far as possible, we will present the deposits in

stratigraphic order, from oldest to youngest. Throughout the trip, we will show the data and reasoning for the spatial correlation of deposits, their numeric age, and the resulting tectonic implications. An important consideration in understanding deformation in this setting is how rocks move horizontally through the subduction wedge. We present geomorphic and stratigraphic data to help resolve the horizontal translation of rocks and thus provide some constraints for shortening over geologic time scale.

As noted, the glacial-interglacial stratigraphy is critical to the analysis of tectonism, and additionally has implications for paleoclimatic processes. Glaciers have descended repeatedly into the coastal lowlands, constructing extensive glacial and glacial-fluvial landforms and depositing a variety of sediments. Abundant organic matter facilitates detailed radiocarbon dating of glacial events, and magnetostratigraphy provides additional age control on older deposits. In the Queets and Hoh River valleys, the glaciogenic sediments include lacustrine-outwash-till sequences. In sea-cliff exposures, a last interglacial wave-cut platform separates early and middle Pleistocene sediments from late Pleistocene sediments. Two older glacial units—the Wolf Creek and Whale Creek drifts—predate the last interglaciation. The Whale Creek drift is of middle Pleistocene age and the Wolf Creek drift is associated with magnetically reversed sediments and is therefore of probable early Pleistocene age. Three additional stratigraphic units—the Lyman Rapids, Hoh Oxbow, and Twin Creeks drifts—document six late Pleistocene glacial advances. The maximum late Pleistocene advance occurred between 54,000 yr B.P. and the last interglacial sea-level highstand (ca. 125,000 yr B.P.), most likely between 55,000 and 75,000 yr B.P. The second glacial maximum occurred ca. 33,000–29,000 cal. yr B.P., while the advance correlative with the ca. 21,000 cal. yr B.P. ice-sheet maximum was far less extensive. Correlation of glacial fluctuations with pollen fluctuations determined from Kalaloch sediments by Heusser (1972) indicates that the glacial advances were driven dominantly by sustained moisture delivery and may reflect insolation-modulated variations in westerly atmospheric flow.

Fluvial terraces are the main source of geologic and Quaternary stratigraphic data used in our tectonic interpretations. Terraces are landforms that are underlain by an alluvial deposit, which in

turn sits on top of a strath, which is an unconformity of variable lateral extent and local relief. Typically, the strath is carved into bedrock, but it can also be cut into older alluvial deposits. At the coast, we recognize straths and their accompanying overlying alluvial deposits, and then show how those features continue upstream into the Clearwater River drainage. The straths and terraces are exposed because there has been active incision of the river into the rocks of the Olympic Peninsula. The most obvious conclusion is that river incision is a response to active rock uplift. But straths and terraces indicate that the incision history of at least one river has not been perfectly steady. There has been variability in external factors, such as climate or tectonics, which has modulated the terrace formation process. What we hope to demonstrate is that the variability in incision process and rate is primarily attributed to climate, but that continued uplift provides the means for long-term net incision of the river into the Olympic landscape.

The first day will involve traveling from Brinnon, on the eastern side of the peninsula, to Hurricane Ridge, in the core, and will end at Kalaloch, on the Pacific Coast. The next day will be mostly dedicated to understanding the coastal stratigraphy in and around Kalaloch, where many of the age constraints for surficial

deposits are located and there are good exposures of the accretionary wedge rocks. The field relationships for permanent shortening of the Olympic wedge will also be explored. The third day will be devoted to the Clearwater drainage and an investigation of terraces of various size, genesis, and tectonic implication. We will consider the myriad of processes that have conspired to construct and preserve the terraces and the possible contributions of both cyclic and steady uplift. The fourth and final day will be spent briefly visiting three geologic features on the way back to Seattle.

## GEOLOGIC SETTING

### Tectonics

The Olympic Mountains are the highest-standing part of the Oregon-Washington Coast Ranges occupying a 5800 km<sup>2</sup> area within the Olympic Peninsula (Fig. 1). The central part of the range has an average elevation of ~1200 m, and reaches a maximum of 2417 m at Mount Olympus (Fig. 1C). The Olympics first emerged above sea level ca. 18 Ma (Brandon and Vance, 1992), and they then seem to have quickly evolved into a steady-state

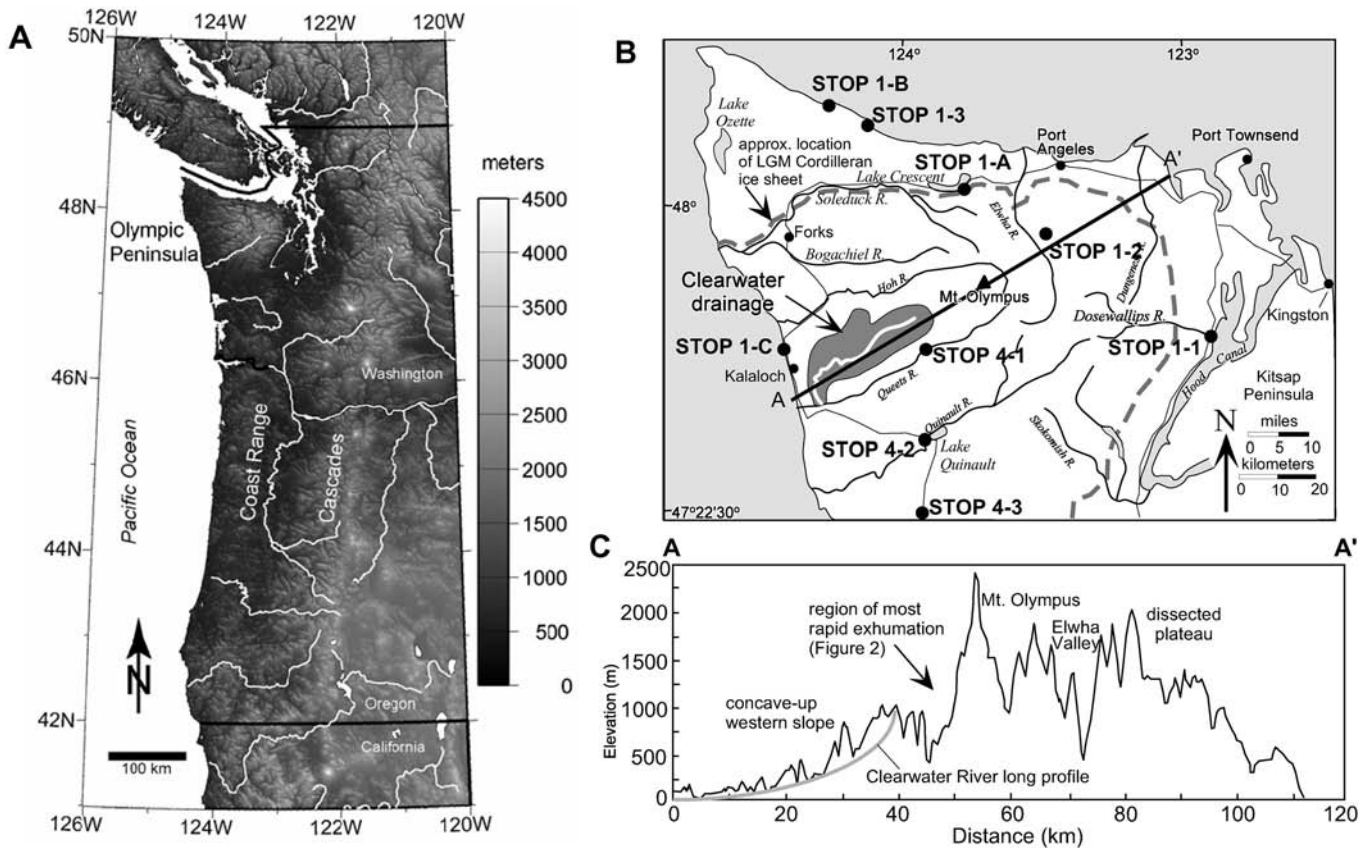


Figure 1. A: Shaded relief digital elevation model of the Pacific Northwest showing the Olympic Mountains in the context of the Coast Ranges. B: Major drainages of the Olympic Peninsula. The gray dashed line marks the southern boundary of the Last Glacial Maximum of the Cordilleran Ice Sheet. Note stops for Days 1 and 4 of the field trip. C: Topographic section across the Olympic Peninsula, parallel to the modern convergence direction (A–A' in B).

mountain range, defined here by rock uplift rates that are closely balanced by erosion rates (Brandon et al., 1998). Fission-track cooling ages indicate that the fastest erosion rates,  $\sim 0.8$  m/k.y., are localized over the highest part of the range (Fig. 2A). Rocks exposed there were deposited and accreted in the Cascadia Trench during the late Oligocene and early Miocene, and then exhumed from a depth of  $\sim 12$ – $14$  km over the past 16 m.y. Present-day rugged relief and high-standing topography are consistent with ongoing tectonic activity, which includes shortening both normal to and parallel to the margin (Fig. 2B). The Cascadia subduction zone underlies a doubly vergent wedge (in the sense of Koons, 1990, and Willett et al., 1993). The change in vergence occurs at the crest of the Oregon-Washington Coast Range, which represents the forearc high. The doubly vergent system includes a prowedge (or proside) that overrides oceanic lithosphere and accretes turbidites of the Cascadia drainage, and a retrowedge (or retroside) that underlies the east-facing flank of the Coast Range (Willett, 1999; Beaumont et al., 1999) (Fig. 3). This usage emphasizes the asymmetry of the underlying subduction zone, defined by subduction of the proplate (Juan de Fuca) beneath the retroplate (North America).

Much of the Cascadia forearc high is underlain by the Coast Range terrane, a slab of lower Eocene oceanic crust (Crescent Formation and Siletz River Volcanics), which occurs as a landward-dipping unit within the Cascadia wedge (Fig. 3A) (Clowes et al., 1987). Accreted sediment that makes up the proside of the wedge reaches a thickness of 15–25 km at the present Pacific Coast (Fig. 3B) and locally extends landward beneath the Coast Range terrane. The Coast Range terrane is clearly involved in subduction-related deformation, even though the rate of deformation is relatively slow when compared with the accretionary deformation occurring at the toe of the seaward wedge. Nonetheless, the Cascadia wedge, by definition, includes all rocks that are actively deforming above the Cascadia subduction zone. Thus, the Coast Range terrane cannot be considered a rigid “backstop,” but instead represents a fully involved component of the wedge.

In the Olympic Mountains, the Coast Range terrane has been uplifted and eroded away, exposing the Hurricane Ridge thrust and the underlying Olympic structural complex (Brandon and Vance, 1992; Stewart and Brandon, 2003) (Fig. 3). The Olympic structural complex is dominated by relatively competent and homogeneous assemblages of sandstone and mudstone, with minor conglomerate, siltstone, and basalt (Tabor and Cady, 1978a, b). A large part of the Olympic structural complex was formed by accretion of seafloor turbidites into the proside of the wedge, starting ca. 35 Ma (Brandon et al., 1998). Where exposed in the Olympics, those accreted sediments are now hard, well-lithified rocks. The steep, rugged topography of the Olympics is supported by both basalts of the Coast Range terrane and accreted sediment of the Olympic structural complex, which suggests that there is little difference in their frictional strength. Uplift in the Olympic Mountains has been driven by both accretion and within-wedge deformation (Fig. 3) (Brandon and Vance, 1992; Willett et al. 1993, see stage 2 of their Fig. 2; Brandon et al., 1998; Batt et

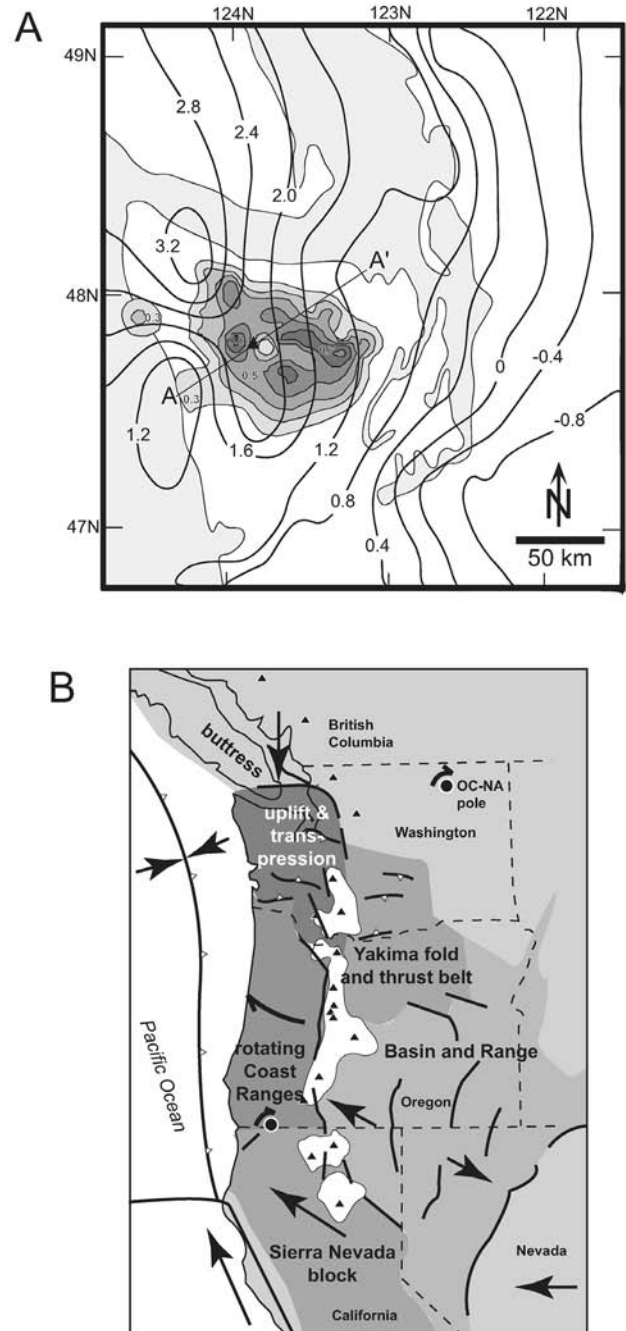


Figure 2. A: Contour map showing short-term uplift rates (solid contour lines) as determined by geodetic measurements (Savage et al., 1991; Dragert et al., 1994) and long-term erosion rates (shaded contour intervals) as determined by fission-track thermochronology (Brandon et al., 1998). Rates are in mm/yr. The preservation of the Quinault and other adjacent near-shore units indicates slow long-term uplift and erosion along the west coast. B: Relative motion of major tectonic blocks in the Pacific Northwest calculated from geodetic data with respect to the Olympic Cascade–North American (OC-NA) pole. Arrows indicate relative block motion. Onshore white polygons and black triangles are volcanic deposits and volcanoes respectively. In this interpretation, uplift of the Olympic Mountains is accomplished by transpression between the Oregon Coast Ranges and a proposed Vancouver Island butress (modified from Wells et al., 1998).

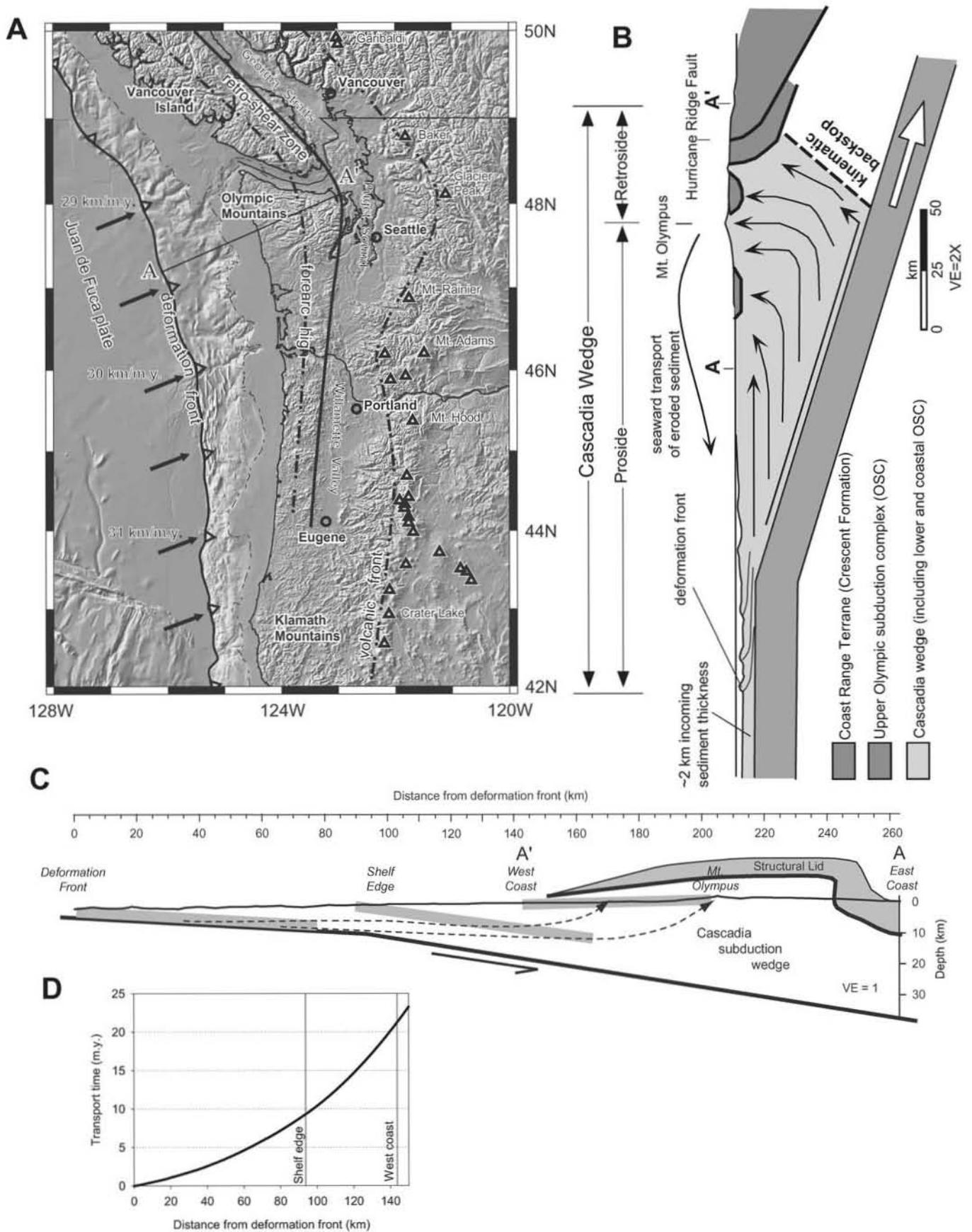


Figure 3. A: Simplified geologic map of the Cascadia convergent margin, modified from Brandon et al. (1998). Beneath the Olympics, the convergence velocity of the Juan de Fuca plate relative to North America is 36 mm/yr at an azimuth of 54°, which is nearly orthogonal to the modern subduction zone (option 2 for Juan de Fuca/Pacific in DeMets et al., 1990, and “NA-PA Combined” in DeMets and Dixon, 1999). B: Schematic section (A–A’ in part A) showing the regional-scale structure of the Cascadia accretionary wedge (after Brandon et al., 1998). VE—vertical exaggeration. C: Inferred displacement path for early Miocene accreted sediments in the Cascadia wedge (Stewart and Brandon, 2003, their Fig. 12). D: Transport time needed to move from the site of initial accretion at the front of the wedge to a location rearward in the wedge (Stewart and Brandon, 2003, their Fig. 13).

al., 2001). Accretion occurs entirely on the proside of the wedge, resulting in decreasing material velocities toward the rear of the wedge. In the Olympics, retroside deformation is marked by folding of the Coast Range terrane into a large eastward-vergent structure (Tabor and Cady, 1978a, b). The upper limb of that fold, which underlies the eastern flank of the Olympics (Fig. 4), is steep and locally overturned, in a fashion similar to the folding illustrated in Willett et al. (1993, stage 2 in their Fig. 2). We infer from the steep topographic slope on the retroside of the wedge that folding is being driven by a flux of material from the proside of the wedge, and that the wedge has not yet begun to advance over the retroside plate (Willett et al., 1993).

Deep erosion and high topography in the Olympics are attributed to an arch in the subducting Juan de Fuca plate (Brandon and Calderwood, 1990; Brandon et al., 1998). The subducting plate is ~10 km shallower beneath the Olympics relative to areas along strike in southwest Washington and southern Vancouver Island (Crosson and Owens, 1987; Brandon and Calderwood, 1990). Stated in another way, the shallow slab beneath the Olympics means that less accommodation space is available to hold the growing Cascadia wedge (Brandon et al., 1998). This situation, plus higher convergence rates and thicker trench fill along the northern Cascadia Trench, has caused the Olympics to become the first part of the Cascadia forearc high to rise above

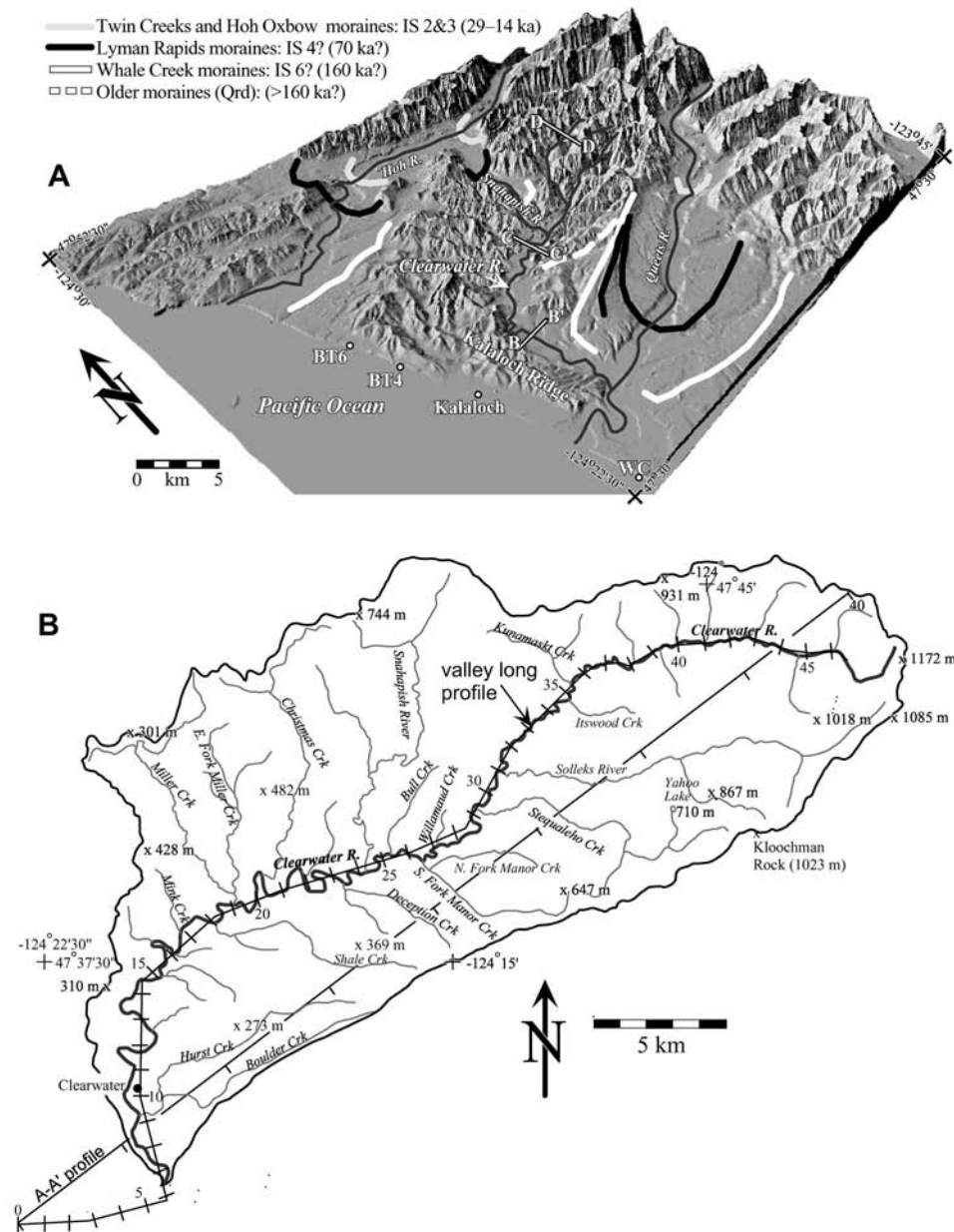


Figure 4. A: Digital shaded-relief image (30-m-resolution digital elevation model) showing the relation of the Clearwater drainage to adjacent drainages and glacial deposits in the western Olympics (glacial data are from Thackray, 1996, 2001; Easterbrook, 1986). BT6, BT4, and WC mark Beach Trail 6, Beach Trail 4, and Whale Creek, where important stratigraphic relationships are exposed along the coast. Profiles B–B', C–C', and D–D' mark cross-valley sections of the Clearwater Valley, as presented in Figure 8. B: Map of the Clearwater drainage. The valley profile is shown as a crooked thin line with ticks marking valley kilometers from the mouth of the Queets River at the coast. The straight section (A–A' in Figs. 1 and 3) lies along the southeast side of the drainage. Final results were projected into A–A', which parallels the local convergence direction for the Cascadia subduction zone. IS— isotope stage.

sea level. The early development of subaerial topography, plus continued accretion and uplift, account for the deep erosion observed in the Olympics. The corollary to this interpretation is that adjacent parts of the forearc high will evolve in the same way, although more slowly because of lower accretionary fluxes and a larger accommodation space for the growing wedge.

### Active Tectonics

There is particular interest in Cascadia regarding the evidence of cyclic deformation related to large earthquakes at or adjacent to the subduction zone (Savage et al., 1981, 1991; Thatcher and Rundle, 1984; Dragert, 1987; Rogers, 1988; Atwater, 1987, 1996; Holdahl et al., 1987, 1989; West and McCrumb, 1988; Darenzio and Peterson, 1990; Atwater et al., 1991; Bucknam et al., 1992; Hynman and Wang, 1993; Dragert et al., 1994; Mitchell et al., 1994). Fundamental to these studies is the distinction between short-term ( $10^2$ – $10^3$  yr) cyclic elastic deformation adjacent to the seismogenic subduction thrust and long-term ( $10^4$ – $10^5$  yr) permanent deformation associated with growth and deformation of the overlying Cascadia wedge. The earthquake cycle is probably partly decoupled from the permanent deformation, so we cannot easily integrate the effects of numerous earthquake cycles and arrive at the final long-term deformation. Furthermore, aseismic ductile flow, occurring within the deeper parts of the Cascadia wedge, probably also contributes to deformation manifested over long time spans.

Holocene deposits preserved in locally subsiding estuaries along the west coast of the Olympics provide good evidence of cyclic deformation related to large prehistoric earthquakes (Atwater, 1987, 1996). Seismogenic slip associated with these earthquakes, both on the subduction thrust and also on upper-plate faults, contributes to long-term deformation of the margin. However, it is difficult to separate elastic deformation, which is created and then recovered during each earthquake cycle, from the permanent deformation associated with fault slip.

Pre-Holocene stratigraphy and structure provide the only records of sufficient duration to separate long-term permanent deformation from earthquake-cycle elastic deformation. For this reason, local active-tectonic studies have focused on deformation of Quaternary deposits and landforms, which are best preserved along the Pacific Coast and offshore on the continental shelf (Rau, 1973, 1975, 1979; Adams, 1984; West and McCrumb, 1988; Kelsey, 1990; Bockheim et al., 1992; Kelsey and Bockheim, 1994; Thackray and Pazzaglia, 1994; McCrory, 1996, 1997; McNeill et al., 1997, 2000; Thackray, 1998). Mud diapirism, which is widespread beneath the continental shelf and along the west coast of the Olympics (Rau and Grocock, 1974; Rau, 1975; Orange, 1990), may be a local factor contributing to the observed deformation of Quaternary deposits.

In contrast, much less is known about the long-term deformation of the coastal mountains that flank the Cascadia margin (Fig. 2A). The development and maintenance of the Oregon-Washington Coast Range as a topographic high suggests that it is an actively deforming part of the Cascadia plate boundary. Diverse

geologic and geodetic data sets seem to indicate shortening and uplift both parallel (Wang, 1996; Wells et al., 1998) and normal (Brandon and Calderwood, 1990; Brandon and Vance, 1992; Brandon et al., 1998) to the direction of convergence (Fig. 2). This relationship is best documented in the Olympic Mountains (Figs. 1, B and C), which, on a geologic time scale ( $>10^3$  yr), seem to be the fastest deforming part of the Cascadia forearc high.

Geodetic and tide-gauge data (Reilinger and Adams, 1982; Holdahl et al., 1989; Savage et al., 1991; Mitchell et al., 1994) indicate that short-term uplift is very fast on the Olympic Peninsula, ranging from 1.2 to 3.2 m/k.y., with the highest rates along the west side of the peninsula (Fig. 2). These high rates probably include a significant component of earthquake-cycle elastic deformation, given that the Cascadia subduction thrust is presently locked. This conclusion is supported by geologic evidence, which indicates insignificant long-term uplift or growth in coastal regions around the peninsula over the past 10 m.y. For instance, exposures of upper Miocene to lower Pliocene shallow-marine deposits locally crop out near modern sea level (Rau, 1970; Tabor and Cady, 1978a; Armentrout, 1981; Bigelow, 1987; Palmer and Lingley, 1989; Campbell and Nesbitt, 2000). These units currently sit within ~200 m of their original depositional elevation, which implies rock-uplift rates less than ~0.05 m/k.y. Slow long-term rock and surface uplift is also consistent with the preservation of extensive middle and lower Pleistocene deposits and constructional landforms along much of the west coast (Thackray and Pazzaglia, 1994; Thackray, 1998).

We use fluvial terraces to examine the pattern and rates of long-term river incision across the transition from the relatively stable Pacific Coast to the actively uplifting interior of the Olympic Mountains. We focus on the Clearwater drainage (Figs. 1B and 4), which remained unglaciated during the late Pleistocene and Holocene, and thus was able to preserve a flight of fluvial terraces, with each terrace recording the shape and height of past long profiles, with the oldest record extending back into the middle Pleistocene.

### Quaternary Stratigraphy

The Quaternary stratigraphy in the lower Queets and Hoh Valleys provides a key framework for understanding terrace age relationships in the Clearwater Valley (Fig. 1). Coastal stratigraphy has been correlated with inland stratigraphy exposed in stream cuts and gravel pits (Thackray, 2001; Pazzaglia and Brandon, 2001), providing detailed age and stratigraphic control. Fill terraces in the lower Clearwater Valley merge with outwash terraces in the lower Queets Valley, and outwash from the lower Hoh Valley breached a low divide in the Snahapish Valley, further influencing the Clearwater terrace stratigraphy. Major outwash terraces in the lower Queets and Hoh Valleys include the Wolf Creek (early Pleistocene?), Whale Creek (middle Pleistocene), Lyman Rapids (55,000–125,000 yr B.P.) and Hoh Oxbow 2 (ca. 33,000–29,000 cal. yr B.P.) terraces. Each outwash terrace surface is underlain by thick (4–15 m) gravel of dominant cobble-pebble sizes, locally containing boulders. Relationships with underlying till, glacial-lacustrine, and bedrock units are exposed locally.

## FIELD RESULTS

### Day 1. Brinnon to Hurricane Ridge to Kalaloch (Fig. 2)

#### *Start. Stop 1-1. Intersection of Route 101 and Dosewallips Valley Road, Brinnon, Washington*

The purpose of this stop is to observe the rocks exposed in the retrowedge of the Olympic accretionary wedge. We will also have the opportunity to observe a Gilbert-delta and discuss glacial and fluvial stratigraphy in the Dosewallips drainage.

A discussion of the Crescent Formation and deformation in the retrowedge is presented above in the Tectonic section. From Brinnon, we gain a good vantage point to envision shortening east of the Hurricane Ridge fault and the topographic crest of the Olympic Mountains.

The fluvial stratigraphy of the Dosewallips drainage has been mapped and incision rates for the eastern part of the Olympic Peninsula are known for a few spot locations (Garcia, 1996). The delta exposed here is related to the Vashon stage glaciation (ca. 14 ka) and is thought to have become emergent by ca. 12.7 ka as a result of both draining of the ancestral Puget Sound, which the delta was building into, as well as isostatic rebound from the retreating Vashon Ice Sheet (Thorson, 1989). Here at Brinnon, there has been 40 m of incision, most of it through Vashon glaciofluvial deposits, which translates to a rate of 3.36 mm/yr. This rate is probably not representative of longer-term tectonic rates as it includes a significant amount of glacio-isostatic rebound. Farther upstream, the glacially polished valley bottom, which is genetically related to drift and other glacial deposits, is deeply incised by the Dosewallips River. At the confluence of the West Fork and main fork of the river (20 km upstream), there has been 19 m of incision and at the confluence with Silt Creek (7 more km upstream), there has been 22 m of incision. Assuming all of this incision is post-Vashon and post-emergence of the delta, the bedrock incision rates are 1.5 and 1.7 mm/yr respectively. Furthermore, a Holocene terrace 15 km upstream near the Elkhorn campground, with a base 5.8 m above the channel was radiocarbon dated at  $3570 \pm 60$  yr B.P., with a corresponding incision rate of 1.6 mm/yr. Accordingly, the postisostatic rebound incision rate for the eastern part of the Olympic Peninsula is between 1.5 and 1.7 mm/yr. There does not appear to be any appreciable increase or decrease in incision rate upstream, nor is there any appreciable change in incision form or process where the Dosewallips River crosses the Hurricane Ridge fault.

Leave parking lot and proceed north on U.S. Rt. 101. The highway cuts through steep topography of the Quilcene Range, all of it underlain by Crescent Formation basalt.

<i>Cumulative Miles</i>	<i>(km)</i>	<i>Description</i>
11.0	(17.7)	Pass through Quilcene, stay north on U.S. Rt. 101.
20.5	(33.1)	Intersection of U.S. Rt. 101 and Rt. 104. Continue on U.S. Rt. 101 toward Port Angeles.

21.2	(34.2)	Crescent Formation exposed in the low outcrop to the right.
22.4	(36.1)	Hills on the left were eroded and smoothed by the continental ice sheet.
41.5	(66.9)	Enter Sequim.
42.2	(68.1)	Intersection with Sequim-Dungeness Way. Proceed straight.
51.1	(82.4)	Low road cut on right and gravel pit on left expose coarse ice sheet outwash.
57.5	(92.7)	Enter Port Angeles.
58.6	(94.5)	Turn left on Race Street, following signs for Olympic National Park south toward Hurricane Ridge.
64.4	(103.9)	Pass entrance station to the park.
68.6	(110.6)	View to the northeast of the Strait of Juan de Fuca.
70.0	(112.9)	Exposures of pillow basalt and pillow basalt breccia, interbedded with bright red, fossiliferous limestone.
71.3	(115.0)	Blue Mountain overlook.
75.5	(121.8)	Cross the Hurricane Ridge fault, which separates the Olympic structural complex from the structurally overlying Crescent basalt and associated forearc basin strata.
76.0	(122.6)	Stop 1-2.

#### *Stop 1-2. Hurricane Ridge Visitor Center, Olympic National Park*

The purpose of this stop is to observe the core of the Olympic Mountains and to discuss thermochronologic data (summarized above) and the feedback between topography, tectonics, and erosion. The Olympic Mountains have been proposed as a range that is in or near flux steady state (Brandon et al., 1998; Pazzaglia and Brandon, 2001; Willett and Brandon, 2002). The topography of the range that is displayed from this vantage point (on a clear day) allows us to think about the roles that elevation, relief, and erosion play in maintaining that flux steady state. The extensive thermochronologic data set for the Olympic Mountains, river suspended sediment data, and river incision rates allow for a comparison of erosion as a function of relief across the range. The Olympic Mountains have a nonlinear relationship between slope gradient and erosion rate which supports the emerging view that erosion rates in tectonically active mountain ranges are adjusted to the rate of uplift, rather than the slope steepness (Brozovic et al., 1997; Montgomery and Brandon, 2002; Fig. 5). Furthermore, the mean slopes calculated for a 10-km-diameter circle across the Olympic Mountain core are relatively invariant despite significant differences in erosion rate or rock type (core vs. peripheral rocks) (Montgomery, 2001). Cross-valley profiles extracted from valleys that have been glaciated, partially glaciated, and nonglaciated show significant differences (Montgomery, 2002). Glaciated valleys draining more than 50 km<sup>2</sup> have two to four times the cross-sectional area and up to 500 m of greater relief than comparable fluvial valleys. These results argue that climate can affect the overall mass flux out of tectonically active ranges like

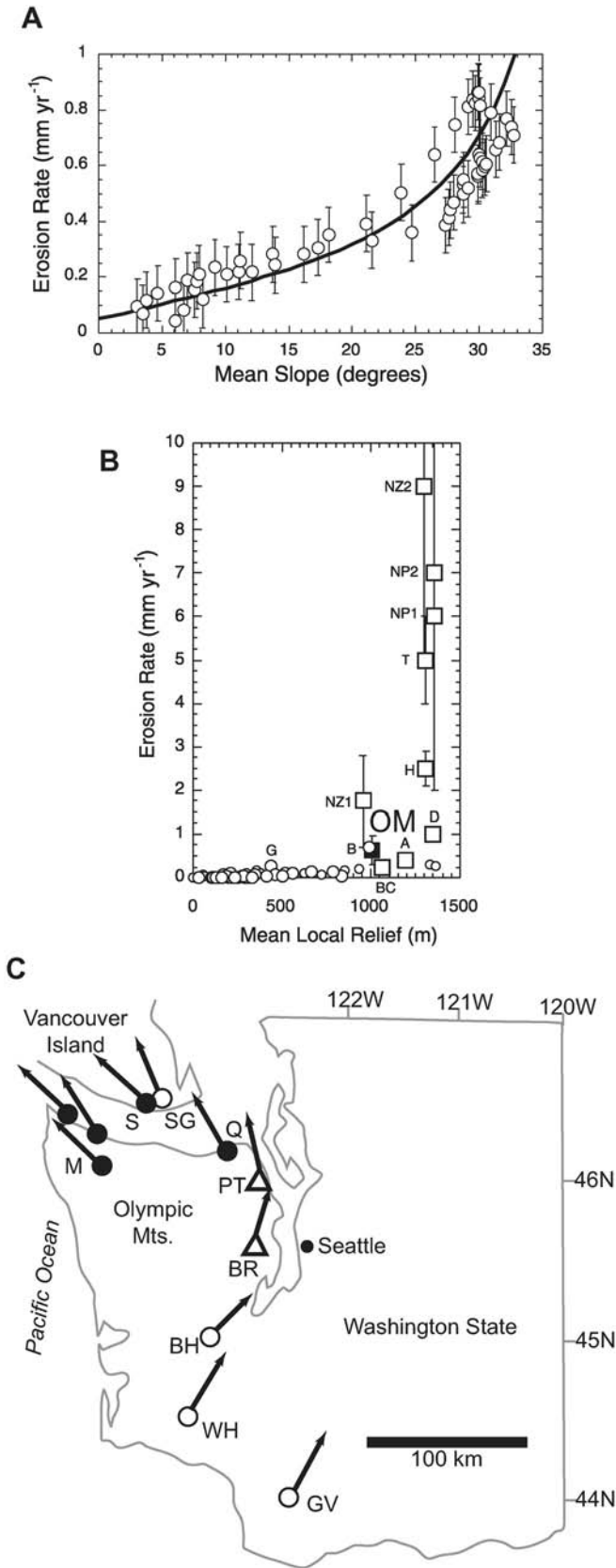


Figure 5. A: Plot of erosion rate data from thermochronometry versus corresponding mean slope determined for a 10-km-diameter circle operating on a 10-m-grid digital elevation model. Error bars represent an uncertainty in the erosion rates of 0.1 mm/yr. The solid line curve shows the predicted nonlinear response of erosion rate to slope angle predicted for landscapes where landslides are important (Roering et al., 2001). B: Plot of erosion rate vs. mean local relief for large, mid-latitude, tectonically inactive basins (the Ahnert, 1970 data, open circles), and large tectonically active basins (filled squares). G—Ganges; B—Brahmaputra; NZ—New Zealand; H—central Himalaya; NP—Nanga Parbat; OM—Olympic Mountains; T—Taiwan; D—Denali; A—Alps. Note location of the Olympic Mountains on this plot. From Montgomery and Brandon (2002). C: Map of western Washington showing paleomagnetic directions and rotations (arrows). Black circles show recently completed results; open symbols show previously published results. BH—Black Hills Volcanics; BR—Bremer-ton basalts; GV—Goble Volcanics; M—Makah-Hoko River Formations; PT—Port Townsend basalts; Q—Quimper and Marrowstone Formations; S—Sooke Formation; SG—Sooke Gabbro of Metchosin Volcanics; WH—Willapa Hills Volcanics. SG after Irving and Massey (1990); rest of figure modified from Beck and Engebretson (1982, Fig. 1).

the Olympic Mountains. Lastly, the elevation of Mount Olympus, or the central massif that contains Mount Olympus, might be partially attributed to an isostatic response to this glacially enhanced erosion (Montgomery and Greenberg, 2000). Calculation of the isostatic rebound at Mount Olympus attributable to valley development ranges from 500 to 750 m (21%–32% of its height) for a 5–10 km effective elastic thickness of the crust. This isostatic effect is one explanation for why the Olympic massif stands above a regional topographic envelope map constructed across the entire range. Alternatively, the transition from fluvial to glacial valleys was more gradual, occurring over 5–10 m.y. as the topography of the Olympic Mountains grew. During the same time, rock uplift would have kept the mean elevation constant, which is limited more by wedge taper than prevailing climate.

Return to Hurricane Ridge Road and retrace route back to Port Angeles.

Cumulative Miles	(km)	Description
87.6	(141.3)	Proceed through entrance gate and down into Port Angeles.
93.4	(150.6)	Turn left onto U.S. Rt. 101 south.
95.8	(154.5)	Leave Port Angeles, begin driving west toward Lake Crescent.
103.2	(166.5)	Cross the Elwha River and pass through the town of Elwha. Rough estimates of the sediment trapped behind the dam, combined with negligible estimates for the rate of chemical denudation, indicate a basin-wide erosion rate of 0.14 mm/yr (Dethier, 1986; B. Stoker, 1991, personal commun.; Brandon et al., 1998).
109.2	(176.1)	Passing Lake Sutherland, notice the predominantly hummocky topography surrounding the lake and ahead. Lake Sutherland has an

- outlet to the east that flows into Indian Creek and ultimately to the Elwha River. Indian Creek is small and underfit in its valley.
- 111.7 (180.2) The road swings to the south and ascends a low, hummocky ridge defining the eastern boundary of Lake Crescent. Enter Olympic National Park and follow the southern shoreline of Lake Crescent.
- 113.9 (183.7) **Optional Stop 1-A. Sledgehammer Point.** The purpose of this optional stop is to observe the Crescent basalts and discuss the origin of Lake Crescent. Lake Crescent is the largest lake on the peninsula. Currently, it has an outlet to the north, through the town of Crescent, directly to the Strait of Juan de Fuca. Its former outlet was back to the east, down the Indian Creek valley. The hummocky topography we passed between Lake Sutherland and Lake Crescent is the debris from a large landslide, derived from the hillside to the north. This natural dam raised the lake level to its present elevation of 176 m (579 ft). The age of the landslide is thought to be early Holocene or late Pleistocene (Tabor, 1975). Lake Crescent is clear, cold, and deep; soundings indicate depths of at least 180 m (600 ft). The lake basin probably reflects both a structural control as well as deep gouging by the continental ice sheet. The pillow basalts exposed in the road cut opposite Sledgehammer Point are vertically bedded with top to the east (Muller et al., 1983).  
Return to U.S. Rt. 101 south.

	<i>Cumulative Miles (km)</i>	<i>Description</i>
122.4	(197.4)	Cross a low divide mantled by glacial deposits but cored by bedrock between Lake Crescent and Soleduck Valley.
126.8	(204.5)	Pass the entrance station to the National Park Service (NPS) Soleduck Valley.
140.4	(226.5)	Sappho, turn right on Rt. 112, head north toward Clallam Bay.
155.5	(250.8)	Clallam Bay. Turn left, remaining on Rt. 112, and head west toward Sekiu.
157.8	(254.5)	Sekiu. Follow signs to Olsen's Resort. Park at the resort and access the coastal exposures.

### **Stop 1-3. Physt Conglomerate and Forearc Basin Rocks of the Olympic Peninsula**

The purpose of this stop is to discuss the forearc basin rocks and present paleomagnetic data related to the direction and magnitude of shortening across the Olympic Peninsula (Fig. 5C). The forearc basin rocks are thick packages of Eocene-Oligocene

deep marine sediments, which apparently were deposited in deep troughs during and after the accretion and docking of the Crescent terrane (Niem et al., 1992). The upper Eocene-Oligocene Lincoln Creek Formation, on the southern flank of the Olympics, spans over 1000 m in thickness (Prothero and Armentrout, 1985). On the north flank of the Olympics, the Pysht Formation (Durham, 1944; Snavely et al., 1978) may be as much as 2000 m thick, although there may be fault repetition of the section. These thick Eocene-Oligocene marine sequences not only record the history of events in the region in the middle Cenozoic, but they also constrain the tectonic models for the Olympics.

Over the past thirty years, numerous paleomagnetic studies have been conducted on many of these rocks. Nearly all the rocks south and east of the Olympic core show a significant post-Oligocene clockwise rotation (Wells and Coe, 1985; Wells, 1990). Until recently, only limited paleomagnetic studies were conducted to the north of the Olympics (Beck and Engebretson, 1982; Symons, 1973; Irving and Massey, 1990), and the results were ambiguous. In the past few years, however, extensive paleomagnetic studies of these rocks have greatly modified our picture of the mid-Cenozoic tectonics of the Olympics.

The most striking result is that the majority of the rocks north of the Olympic core complex show a post-Oligocene *counterclockwise* tectonic rotation, the opposite of the clockwise rotations reported east and south of the Olympics. On the northwest corner of the Olympic Peninsula, the upper Eocene-Oligocene Hoko River and Makah Formations show a counterclockwise rotation of  $\sim 30 \pm 3^\circ$  (D.R. Prothero, 2003, personal commun.). On the northeastern corner of the Olympic Peninsula, the upper Eocene-Oligocene Quimper sandstone and Marrowstone shale show a counterclockwise rotation of  $42 \pm 9^\circ$  (D.R. Prothero, 2003, personal commun.). Across the Strait of Juan de Fuca, on the southern tip of Vancouver Island, the upper Oligocene Sooke Formation yields a counterclockwise rotation of  $\sim 25 \pm 10^\circ$  (D.R. Prothero, 2003, personal commun.), consistent with earlier results reported by Symons (1973) and Irving and Massey (1990) for the underlying Eocene Mechosin Volcanics. Although the Sooke Formation is north of the Canadian border, it is tectonically part of the Olympics, since it lies to the south of the Leech River fault.

The only exceptions to this trend are the result reported from the Pysht and Clallam Formations along the central coast of the Olympics. The Oligocene Pysht Formation produces a clockwise tectonic rotation of  $\sim 49 \pm 6^\circ$  (Prothero et al., 2001), and the overlying lower Miocene Clallam Formation yields a clockwise rotation of  $45 \pm 15^\circ$  (Prothero and Burns, 2001). This suggests that the tectonics of the north coast of the Olympics are more complex than previously expected, and we are currently analyzing these data to find an explanation for this apparent contrary rotation.

However, the overwhelming counterclockwise sense of rotation on rocks from the Quimper Peninsula in the northeast to Makah Bay on the northwest demands some sort of explanation. Tabor and Cady (1978b) commented on the horseshoe-shaped pattern of the Tertiary rocks wrapped around the Olympic core, and postulated that they had undergone some sort of oroclinal bending

around the Olympics as they pushed eastward. We favor a model similar to this, where the eastward movement of the Olympic core “bulldozes” the rocks in its path into a curved pattern. Such bulldozing would rotate the rocks north of the core in a counterclockwise sense, and those south of the core in a clockwise sense.

Return to Olsen’s Resort and Rt. 112. Proceed west on Rt. 112 to optional stop 1-B, otherwise, retrace route out to Sappho and U.S. Highway 101.

<i>Cumulative</i>		<i>Description</i>
<i>Miles</i>	<i>(km)</i>	
157.8	(254.5)	Return to Rt. 112 and proceed toward Neah Bay.
165.7	(267.3)	Shipwreck Point. This is <b>Optional Stop 1-B</b> . The purpose of this stop is to observe turbidites and olistostromes in the forearc sedimentary rocks. A walk to the east along the coastal outcrops from Shipwreck Point leads to exposures of the Janssen Creek Member of the Makah Formation, with its huge turbidites and olistostromes plainly visible. These rocks are also rich in early whale fossils, the mysticetes type that are transitional between tooth and baleen groups. Return to Sekiu and then to Sappho and U.S. Highway 101.
191.0	(308.1)	Intersection with U.S. Rt. 101, turn right.
202.6	(326.8)	Cross Soleduck River and the southern boundary of Vashon-age drift from the Juan de Fuca lobe of the continental ice sheet.
205.3	(331.1)	Enter Forks, the largest town on the western Olympic Peninsula.
210.9	(340.2)	Cross the Bogachiel River.
216.5	(349.2)	Ascend a low divide between the Bogachiel and Hoh River drainages underlain by a large lateral moraine complex of the Hoh Valley. The moraine here forms the northern divide of the lower Hoh River valley. A minimum age for the moraine of $30,000 \pm 800$ yr B.P. was obtained from organic material in a bog ~0.5 km to the southwest (Heusser, 1974). Approximately 6 km upstream from this point, another well-defined moraine ridge has yielded a basal bog minimum age of $18,800 \pm 800$ yr B.P. (Heusser, 1974). A nearly identical age from peat clasts in overbank silt was obtained in the lower Bogachiel drainage (Heusser, 1974, 1978). The interstadial peat site (Heusser, 1978), 60 m above the Bogachiel River, exhibited 85 cm of peat underlain by more than 2 m of unweathered diamicton and 2 m of brown, compact, thoroughly weathered till. The top of the peat has a reported age of 59,600 yr B.P. (essentially infinite). Pollen in the interstadial peat indicated subalpine forests
219.0	(353.2)	Pass entrance road for the Hoh Rain Forest.
220.8	(356.1)	Cross the Hoh River. The Hoh River supports one of the last remaining salmon runs on the peninsula. The road now bends to the southwest and heads for the coast.
232.2	(374.5)	U.S. Rt. 101 bends directly south, enters Olympic National Park, and parallels the coast.
234.0	(377.4)	<b>Optional Stop 1-C. Destruction Island viewpoint.</b> The purpose of this stop is to observe the Pacific Coast and set the stage for the next day’s tour of glacial and tectonic topics.
240.5	(387.9)	Turn right into Kalaloch Lodge parking lot. This is the end of Day 1, and headquarters for the remainder of the field trip.

being succeeded by tundra and park-tundra type floras. The pollen in the bog suggests a rise in arboreal species including hemlock and pine at 30 ka, followed by tundra and park-tundra types by 20 ka, a rise of Sitka spruce and alder between 20 and 10 ka, maximum percentages of alder in the early Holocene, and finally to a modern palynoflora dominated by western hemlock. The glacial stratigraphy and palynostratigraphy suggests (1) a pre-Wisconsinan ( $>59,600$  yr B.P.) and early Wisconsinan ( $<59,600$  yr B.P.) glaciation that crossed the divide between the lower Hoh and Bogachiel drainages, extending all the way to the present coast, and (2) a late Wisconsinan (Fraser, ~18 ka) glaciation that extended to within 6 km east of this point in the Hoh Valley. The upper Hoh Valley currently supports active cirque glaciers. A goal of the Day 2 itinerary is to revisit the glaciation history since Heusser’s important contributions 30 years ago.

219.0 (353.2) Pass entrance road for the Hoh Rain Forest.  
220.8 (356.1) Cross the Hoh River. The Hoh River supports one of the last remaining salmon runs on the peninsula. The road now bends to the southwest and heads for the coast.  
232.2 (374.5) U.S. Rt. 101 bends directly south, enters Olympic National Park, and parallels the coast.  
234.0 (377.4) **Optional Stop 1-C. Destruction Island viewpoint.** The purpose of this stop is to observe the Pacific Coast and set the stage for the next day’s tour of glacial and tectonic topics.  
240.5 (387.9) Turn right into Kalaloch Lodge parking lot. This is the end of Day 1, and headquarters for the remainder of the field trip.

## Day 2. Coastal Exposures Near Kalaloch, Olympic National Park, Moses Prairie Paleo-Sea Cliff and the Record of Horizontal Shortening, Hoh Formation, Glaciation in the Hoh Valley (Fig. 6)

### Start, Kalaloch Lodge

Walk to the beach overlook for a brief overview. Kalaloch and the entire field-trip route lie in the west-central part of the Olympic Peninsula, between two large drainages, the Hoh and Queets Rivers, that drain the northwest, west, and southwest flank of Mount Olympus (Figs. 1B and 3A). The Clearwater River is tucked away between these two master drainages, and we use the fluvial and glacial deposits of the Hoh and Queets Rivers to constrain the ages of terraces in the Clearwater drainage (Fig. 7). The Olympic coast here is a constructional feature underlain by glaciofluvial deposits. It lacks the distinct, uplifted marine terraces characteristic of Cascadia in Oregon and northern California, although the effects of glacio-eustasy and coastal tectonics cause a major unconformity

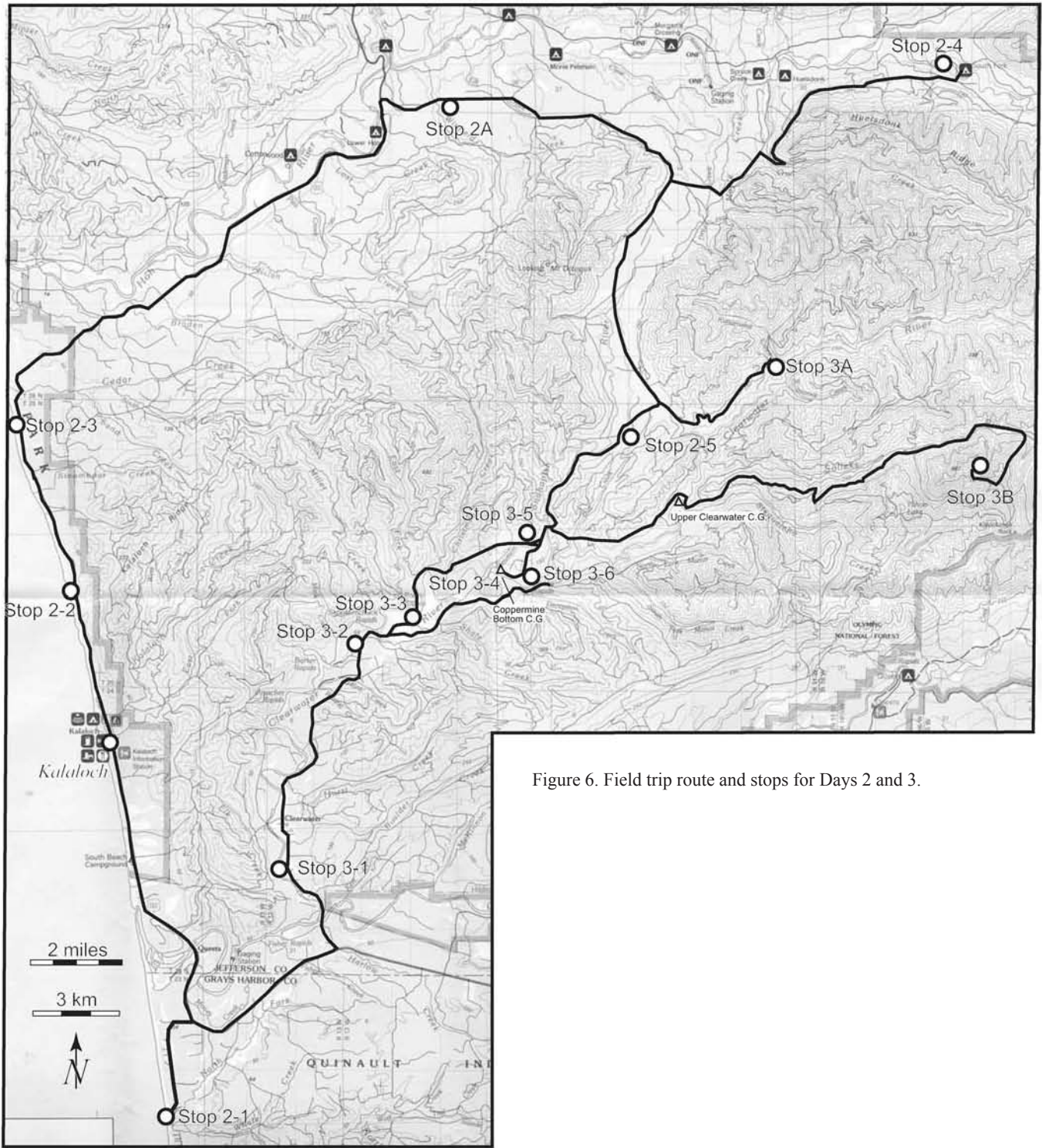


Figure 6. Field trip route and stops for Days 2 and 3.

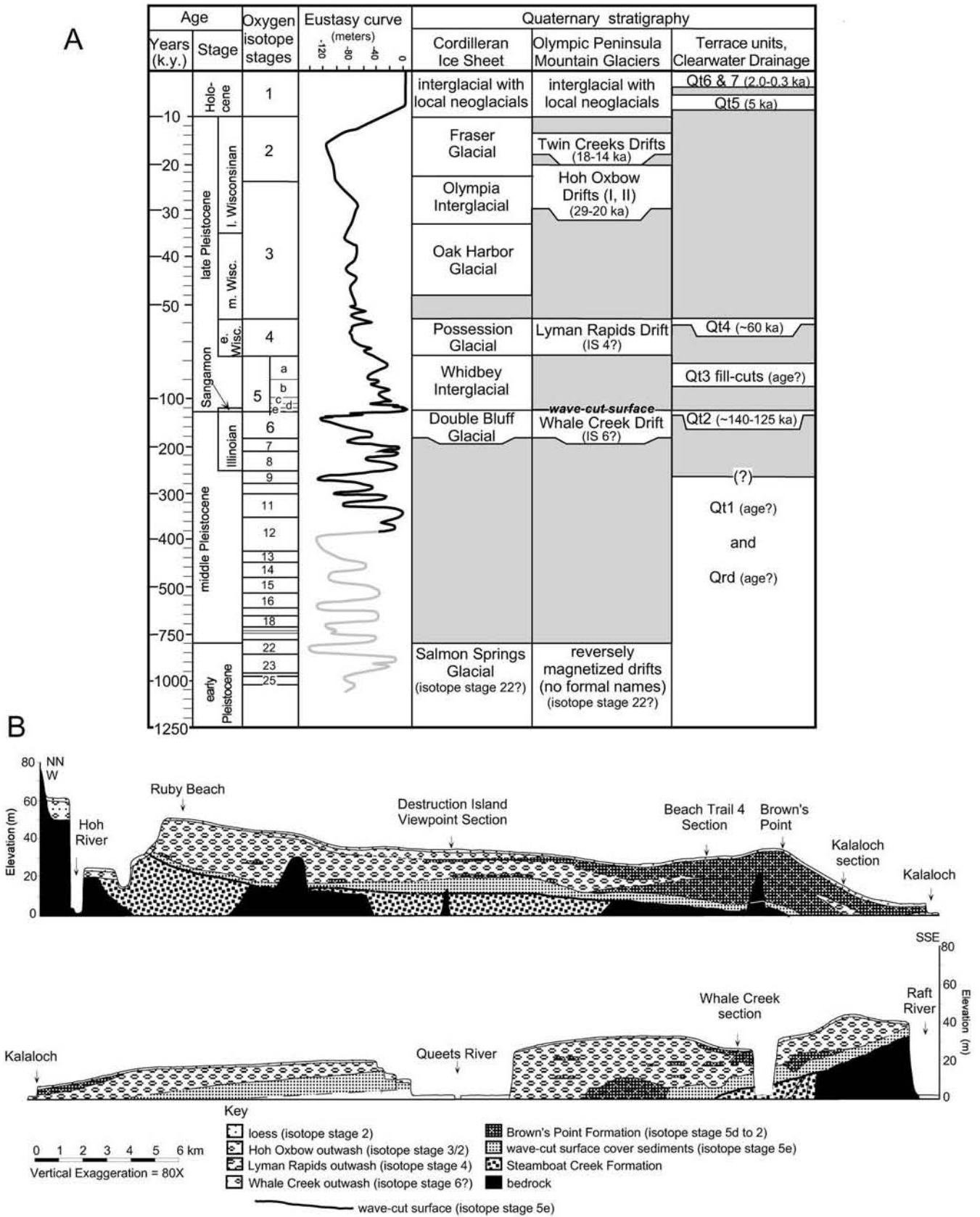


Figure 7. A: Regional stratigraphic correlations for glacial and fluvial deposits in the western Olympic Peninsula and surrounding regions. Note the variable scaling in the time axis. Eustasy curve is from Chappell et al. (1996) for 0–140 ka, and Pillans et al. (1998) for 140–300 ka. The next column shows deposits associated with advances and retreats of the Cordilleran Ice Sheet in Puget Sound, as synthesized by Easterbrook (1986). The next column shows the stratigraphic record of alpine glaciation in the western Olympics, based on the work of Thackray (1996, 2001). We have excluded his drift unit, called Hoh Oxbox 0 and estimated to be 39–37 ka, because it is based solely on an isolated sequence of lake sediment. The final column shows terrace stratigraphy in the Clearwater Valley as determined by work presented here. B: Compiled stratigraphy of the Olympic Peninsula west coast sea cliff from Hoh Head to Whale Creek (from Thackray, 1996).

in the coastal stratigraphy. Both stratigraphy and correlation of the widespread unconformity indicate active tectonic deformation in the form of a broad (tens of km) fold with an axis oriented roughly northeast or parallel to the direction of convergence (Rau, 1973; McCrory, 1996; Thackray, 1998). The mouth of the Queets River marks the approximate southern limb of a syncline centered on Kalaloch, and the mouth of the Hoh River marks the northern limb of the syncline. The significance of this syncline and all associated broad folding of Quaternary deposits at the coast is in the general lack of significant rock uplift and the comparatively small amount of northerly shortening in comparison to the large amount of shortening and uplift in the direction of plate convergence. The relative tectonic stability of the coast is also supported by preservation of early Pleistocene glaciofluvial deposits, as well as Miocene-Pliocene neritic shelf-basin deposits like the Quinault and Montesano Formations that outcrop at or near sea level. However the precise paleoelevation history of such ancient deposits, like the Quinault and Montesano Formations, must be viewed in the context of the large but unknown degree of horizontal translation they have experienced because of wedge shortening.

Exit Kalaloch and turn right.

Cumulative Miles	(km)	Description
2.7	(4.4)	South Beach campground is to the right. The 20 m tread here has been dated as $4570 \pm 60$ radiocarbon yr B.P. The dated material unconformably overlies late Pleistocene alluvium (Lyman Rapids outwash).
4.9	(7.9)	Cross the Queets River. Highway 101 is following a big meander loop of the Queets River. To the left are several late Pleistocene to Holocene terraces and sloughs. To the right are treads of the 30 m terrace. Engineering borings for the bridge show that the alluvium is thin (6 m); there is no deep, filled thalweg beneath the river channel. In other words, the river is essentially running over a low-relief bedrock strath.
6.6	(10.6)	Turn right and stay straight on the dirt road. This is now Quinault Nation land, and access permission is needed from the tribal government in Tahola. Moses Prairie is on the left, following the valley of the North Fork Whale Creek.
7.1	(11.5)	Stay left on the main dirt road, proceed south, remain on the 30 m terrace.
8.9	(14.4)	Stop 2-1.

**Stop 2-1. Whale Creek**

There are two objectives at this stop. The first is to observe the southern limb of the Kalaloch syncline and deformed Quaternary stratigraphy. Follow the old track along the north bank of the creek and cross driftwood field to the beach. Walk north ~200 m to the first exposures lying parallel the coast (Fig. 8).

**Whale Creek**

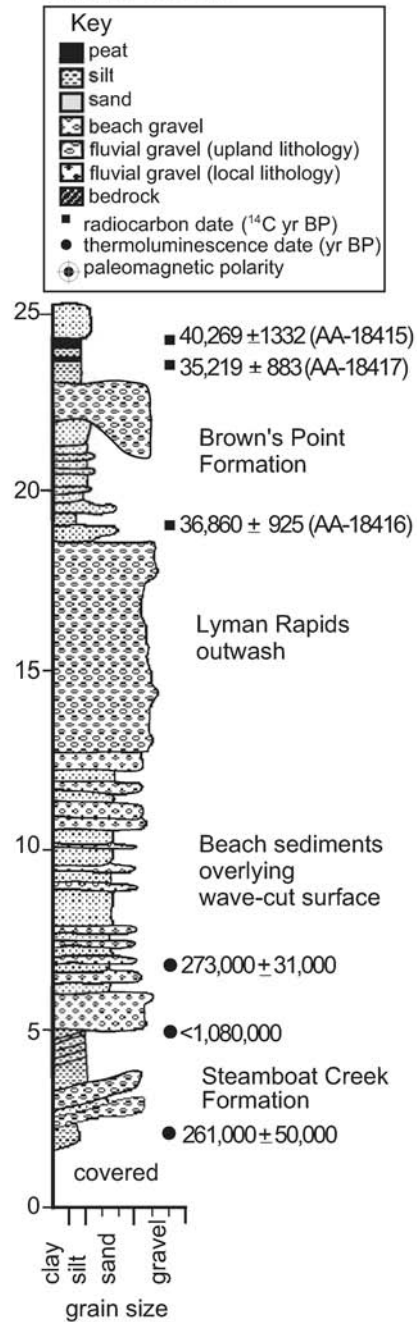


Figure 8. Whale Creek section.

The stratigraphic sequence in this area is broadly similar to that at Destruction Island viewpoint and similarly fills a 1.5-km-wide area seaward of a paleoshoreline. The wave-cut surface here is not marked by a boulder lag, but is obvious as an angular unconformity. It has an apparent dip of ~3° north in this immediate area. Strata underlying the wave-cut surface have an apparent dip of 11° north. The wave-cut surface descends to beach level

a short distance north of this first exposure. Horizontally bedded beach deposits overlie the wave-cut surface and form the base of the exposed sequence north of that location. Approximately 1 km farther north, the beach deposits abut against a 5-m-deep gravel-filled channel. The gravel fill is capped by ~1 m of silt and peat, which thickens northward. Two kilometers north of Whale Creek, the silt/peat sequence is 7.5 m thick, including a 2-m-thick gravel bed in the middle of the sequence. These sediments likely accumulated during latter substages of the last interglaciation.

The sequence above the wave-cut platform at the first exposure north of Whale Creek consists of 6.3 m of outwash and 6.3 m of fine-grained sediments. The latter consist of interbedded fine sand and silt, fining generally upward to silt with peat interbeds. A pebble-gravel bed cuts that fining upward sequence. Pollen spectra from this fine-grained sequence indicate cooling climatic conditions, from stable, mild conditions (at base) to cold-climate conditions represented by an alpine assemblage at the top (Florer, 1972). The sequence yielded three radiocarbon dates of 35–40 ka.

If time and tides permit, return to Whale Creek and cross to the south side. Walk ~0.5 mi south to the prominent exposure. On the way, note prevalence of slumping. The green, beach-side

cabin (if still in existence) formerly sat on a level patch of ground about half way up the cliff. In the early 1990s the hillside mobilized, lowering the cabin to beach level and rotating it 90°. This spectacular outcrop provides clues to the style of deformation on the south limb of the Kalaloch syncline. Bedding attitudes in the older sequence (below the wave-cut surface) steepen progressively from north to south across the outcrop, from ~18° north to nearly 90°. Apparent unconformities separate beds of different attitudes. These relationships are suggestive of a fault-propagation fold at the tip of a buried thrust fault, the upper portion of the fold having been removed during wave-cut surface formation. The progressively steeper dips suggest that the fault was active through the period in which the strata were deposited. Such a structure may be responsible for the relatively steep inclination of the wave-cut surface on this limb of the Kalaloch syncline.

The second objective is to observe the paleo-sea cliff, relate the 30 m and 60 m coastal treads to glaciations in the Hoh and Queets River valleys, and discuss how the paleo-sea cliff tracks the horizontal motion of rocks and shortening of the wedge (Fig. 9). For a detailed discussion, see Willett et al. (2001) and Pazzaglia and Brandon (2001).

Retrace route out to U.S. Rt. 101.

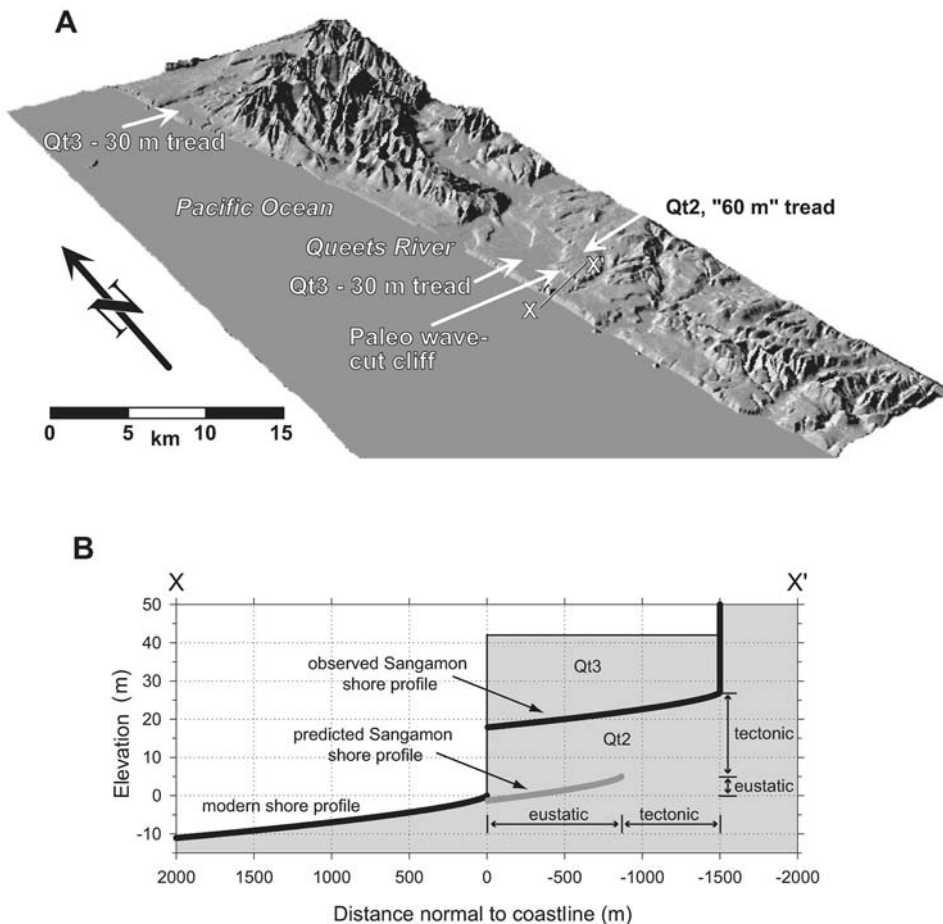


Figure 9. A: Digital shaded relief showing the buried Sangamon sea cliff. The cliff shows up as subdued scarp that parallels the coast at a distance 1500 m inland. The feature is visible in the image from ~15 km south to ~5 km north of the Queets River. B: A schematic cross section of the modern shoreface and sea cliff and the buried Sangamon sea cliff at the mouth of the Queets River. The section X–X' follows A–A'; it has an azimuth of 54°, parallel to the plate convergence direction (Pazzaglia and Brandon, 2001).

Cumulative Miles	(km)	Description
11.2	(18.1)	Turn left on U.S. Rt. 101.
18.4	(29.7)	NPS Kalaloch campground is on the left. Highway 101 hugs the coast, traveling on a tread ~20 m in elevation. This tread is underlain by late Pleistocene alluvial and eolian deposits as well as Holocene marsh deposits.
20.3	(32.7)	Pass Brown's Point (Beach Trail 3) and rise onto a 30 m terrace tread. This 30 m terrace is well preserved along the coast and will figure significantly into the stratigraphic story.
21.1	(34.0)	Stop 2-2.

#### Stop 2-2. Beach Trail 4

The purpose of this stop will be to see the rocks of the Cascadia wedge and begin developing the stratigraphic framework of the Quaternary deposits by observing the 122 ka wave-cut unconformity. A key point is that rocks exposed at the coast may have moved northeastward into the coast, with little to no uplift. Park in the NPS parking lot and descend the trail leaving from the southeast corner of the lot and go to beach level.

The bedrock exposed here consists of turbidites of the Miocene Hoh Formation (Fig. 10A). These rocks were deposited on the continental slope in at least 2 km of water and have been uplifted here to sea level. More importantly, the Hoh Formation was laid down 50–100 km west of its current position and has since followed a largely horizontal trajectory to the present Olympic coastline (Fig. 3B). Stewart and Brandon (2003) have shown, using fission-track grain ages from detrital zircons, that the Hoh Formation, which is also called the coastal unit of the Olympic structural complex, was deposited between ca. 24 and 16 Ma in water depths greater than 2000 m, which would correspond to the abyssal Cascadia basin, west of the modern Cascadia subduction zone. These rocks were accreted at the front of the Cascadia wedge, which is presently located 100 km west of our current position, and then slowly transported landward within the wedge (Fig. 3B), only reaching the coast at present. Figure 3C shows a reconstruction of this transport through the wedge, and Figure 3D shows the estimated history of landward translation.

The nearly vertically bedded bedrock is planed off ~2.7 m above mean sea level by a wave-cut unconformity. A thin boulder lag locally lies atop the unconformity, and it is superceded by gray pebbly beach sand texturally and structurally identical to the modern exposed shoreface. Exposures along the trail leading to the beach clearly show the unconformity continuing west under the 30-m coastal terrace (Fig. 9A). Cylindrical borings in the Hoh beneath the unconformity are interpreted as being shaped in part by pholad clams. The stratified sand, gravel, and peat overlying the beach deposits are part of the Brown's Point Formation (Heusser, 1972; Thackray, 1998; Fig. 10B). Gravel clasts in this deposit tend to be weathered and their provenance is consistent with a local source, most likely Kalaloch Ridge directly to the west, rather than the Hoh or Queets Rivers, whose deposits tend

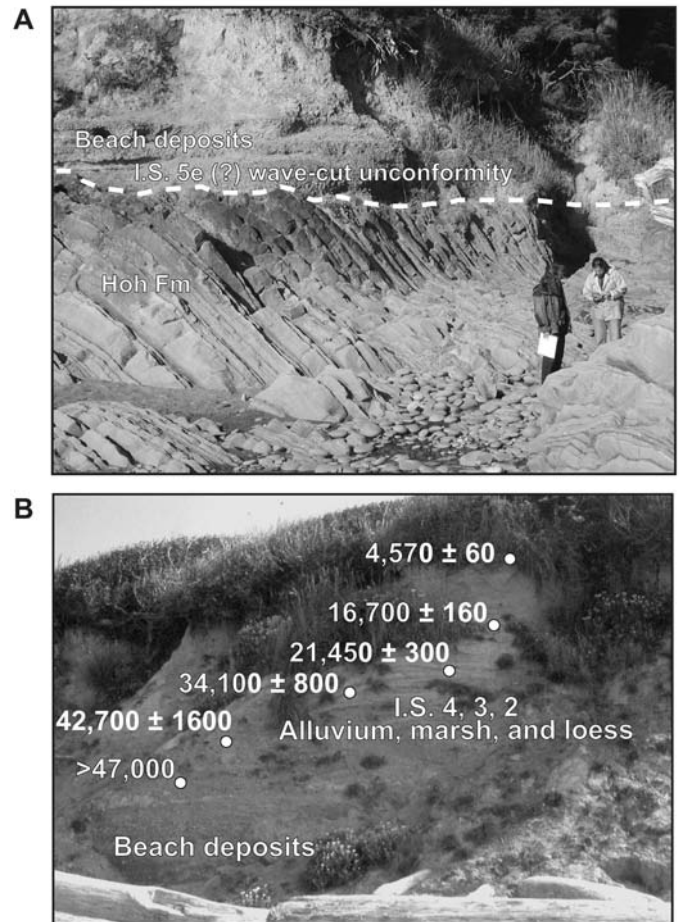


Figure 10. A: Photograph of the bedrock and wave-cut unconformity exposed at Beach Trail 4. B: Annotated photograph of the Quaternary stratigraphy and numeric ages typical of the Brown's Point Formation in the vicinity of Beach Trail 4 (from Thackray, 1996). I.S.—isotope stage.

to be less weathered. The Brown's Point Formation seems to represent a long period of fluvial, glaciofluvial, and marsh-type sedimentation. The base of the unit directly above the beach sands is radiocarbon dead, but stratigraphically higher deposits have progressively younger radiocarbon ages (Heusser, 1972; Thackray, 1996). The youngest age comes from ~6 m below the terrace tread and is  $16,700 \pm 160$  radiocarbon yr B.P.

The wave-cut unconformity here (Fig. 10A) is a key stratigraphic horizon, which can be traced for 80 km along the coast. It does not remain at the elevation viewed here. At Kalaloch, the unconformity is below sea level and not exposed. It rises to a maximum of 52 m above sea level south of the mouth of the Queets River. The average elevation between the mouth of the Hoh and Queets Rivers is 11 m. Deposits both above and below the unconformity are radiocarbon dead. At this stop we propose that the unconformity represents a wave-cut surface, produced during eastward migration of a shoreface during the last major interglacial eustatic highstand, at 122 ka (isotope stage 5e). We will develop the evidence at subsequent stops.

Cumulative Miles	(km)	Description
23.3	(37.6)	Cross Steamboat Creek.
25.2	(40.6)	Turn left. Stop 2-3.

### Stop 2-3. Ruby Beach (lunch Stop)

The purposes of this stop will be to observe the Quaternary deposits above and below the wave-cut unconformity, key points for numeric ages of the deposits, and to observe the Hoh Formation. We follow the field observation of these units with a map-based correlation to glacial deposits in the Hoh and Queets River valleys. Park in the NPS lot and follow the trail to the beach. The exposures between Beach Trail 6 and Ruby Beach have changed significantly in recent years because of landsliding and coastal erosion.

The wave-cut unconformity is higher here, ~12 m above sea level, and is marked by a boulder lag (Fig. 11). The deposit below the unconformity was first named and described by Florer (1972) as the Steamboat Creek Formation. It is a complexly interbedded sequence of till, lacustrine deposits, glaciofluvial outwash, and sand dunes, which has yielded only infinite radiocarbon ages (below the detection limit for radiocarbon). Samples collected from lacustrine beds within this unit by Pazzaglia and Thackray, and analyzed by H. Rowe and J. Geissman at the University of New Mexico, show both normal and reversed polarities (Thackray, 1996). At this site in particular the polarity of the sample is reversed, indicating an age greater than 780 ka, the most recent reversal. Beach deposits and associated peat overlie the unconformity and are succeeded by predominantly glaciofluvial outwash sourced from the Hoh drainage. The outwash within 15 m of the unconformity is interbedded locally with peaty beds that have returned radiocarbon-dead ages of >33.7 and >48 ka (Florer, 1972). Closer to the terrace tread, in a bed locally separating two outwash units, finite radiocarbon ages of  $36,760 \pm 840$  and  $28,352 \pm 504$   $^{14}\text{C}$  yr B.P. have been determined on woody material by Thackray (1996). The interpretation of these ages suggested by Thackray (1996, 2001) is that the outwash and peat-rich sediments directly above the wave-cut unconformity are correlative to a marine isotope stage 4 (or possibly 5d, b) alpine glaciation (Lyman Rapids advance) and that the upper outwash was deposited by streams during isotope stage 3.

The new landslides here between Beach Trail 6 and Ruby Beach expose mud diapirs that are both onlapped by and that pierce the Steamboat Creek Formation (Rau and Grocock, 1974; Rau, 1975; Orange, 1990).

Return to the base of the trail and assemble for a view of Destruction Island. The broad topographic and structural low between the mouth of the Hoh and Queets Rivers filled with sediment from those two point sources, as well as from small streams draining Kalaloch Ridge (Fig. 9A). The center of the low near Kalaloch has more fine-grained sediment than do the regions proximal to the big river mouths. The general model is that the Queets and Hoh Rivers have periodically been point sources that built broad fans in front of the river mouths, spilling laterally

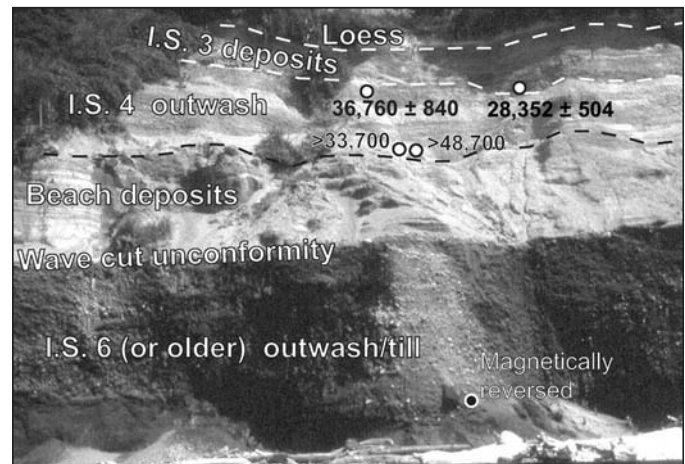


Figure 11. Annotated photograph of the Quaternary stratigraphy exposed between Beach Trail 6 and Ruby Beach (from Thackray, 1996). I.S.—isotope stage.

into the Kalaloch low. The fans formerly extended far west of the current coast. The top of Destruction Island 5 km offshore (20 m elevation) is correlative to the 30 m tread here at the coast, and the flanged base of Destruction Island that sits only 1 m above mean tide level is the westward continuation of the wave-cut unconformity. The level of the fan tread, represented by the 30 m terrace seen all morning of Day 2, must reflect a significant amount of vertical aggradation rather than tectonic uplift. The preservation of the isotope stage 5e unconformity and ca. 800 ka Pleistocene deposits in the outcrop below this viewpoint attest to the relative tectonic stability of the coast.

The most likely time for major periods of fan aggradation on a generally tectonically stable coastal setting is during a cycle of alpine deglaciation, as the river valleys are liberating a high sediment flux at the same time sea level is rising. It is difficult to imagine how the observed degree of aggradation could have occurred during a relative sea level low on a coast not undergoing rapid vertical uplift. Furthermore, map relationships show how the coastal terrace treads can be traced more or less continuously up the Hoh and Queets Valleys to heads of outwash (moraines). The general glacial stratigraphy of the Hoh and Queets Valleys (Thackray, 1996, 2001; Fig. 6) records a major isotope stage 4 alpine glaciation (55–125 ka, Lyman Rapids drift), which was responsible for the large body of outwash above the wave-cut unconformity and the construction of the 30 m terrace at the coast. Older alpine glacial periods, such as isotope stage 6 (150 ka, Whale Creek drift), are represented locally by the deposits below the wave-cut unconformity. However, there are clearly deposits older than isotope stage 6 below the unconformity, and these have a landward equivalent in various upland gravels, a Queets Valley moraine-outwash sequence called the Wolf Creek drift. Deposits of isotope stage 3 and 2 alpine glacial periods are under-represented at the coast because of the relative small size of the glaciations. However, isotope stage 3 outwash is represented in

the upper portion of the sequence south of Cedar Creek (Ruby Beach). Meltwater streams appear to have breached a divide at the head of Cedar Creek, permitting an outwash fill to be deposited in that valley and seaward of the last-interglacial seacliff.

<i>Cumulative Miles (km)</i>	<i>Description</i>
25.3 (40.8)	Return to vehicles, exit parking lot, and turn left (north) onto U.S. Rt. 101.
27.0 (43.5)	U.S. Rt. 101 follows the Hoh River upstream. The road is built on a late Pleistocene outwash plain of valley glaciers with heads of outwash located several kilometers ahead in the direction of travel.
38.5 (62.1)	U.S. Rt. 101 turns to the north and ascends moraines of the Hoh Oxbow drift.
39.3 (63.4)	Turn right onto the Snahapish-Clearwater Road. The road climbs a bedrock-till high that represents the Hoh Oxbow 2 glacial limit (29,000–26,000 <sup>14</sup> C yr B.P.) (Thackray, 2001).
40.7 (65.6)	Cross Winfield Creek.
41.0 (66.1)	Slow, turn right on dirt road to <b>Optional Stop 2-A. Department of Transportation gravel pit</b> . The purpose of this stop is to observe the stratigraphy, sedimentology and soil development (Fig. 12) in the Hoh Oxbow (ca. 20 ka) outwash.
41.0 (66.1)	Return to the Snahapish-Clearwater Road, proceed east.
44.0 (71.0)	Dead-ice moraine on right. Heusser (1974) obtained a 14,480 ± 600 yr B.P. radiocarbon date on peat from a bog on the moraine, as well as a 15,600 ± 240 yr B.P. date from a bog lying 0.9 mi northwest.
46.0 (74.2)	Eocene-Oligocene bedrock on right (Tabor and Cady, 1978a), Hoh Oxbow 3 lateral moraine to left.
46.2 (74.5)	Turn left and begin to cross a broad, flat plain underlain by outwash and drift. Heusser (1974) reported an 18,800 ± 800 yr B.P. radiocarbon date on peat from a bog 1.6 mi north.
48.5 (78.2)	Turn right, cross Owl Creek.
48.8 (78.7)	Make a sharp left turn and ascend the nose of Huelsdonk Ridge. Note numerous debris flows deposits and stream channels affected by debris flows that originated in the short, steep tributaries draining this ridge to the north into the Hoh Valley.
53.5 (86.3)	Turn left, cross the South Fork of the Hoh, then turn right into the South Fork Hoh campground. Trail to the South Fork Hoh glacial exposures begins on the south side of the bridge and proceeds west (downstream).
53.8 (86.8)	Stop 2-4.

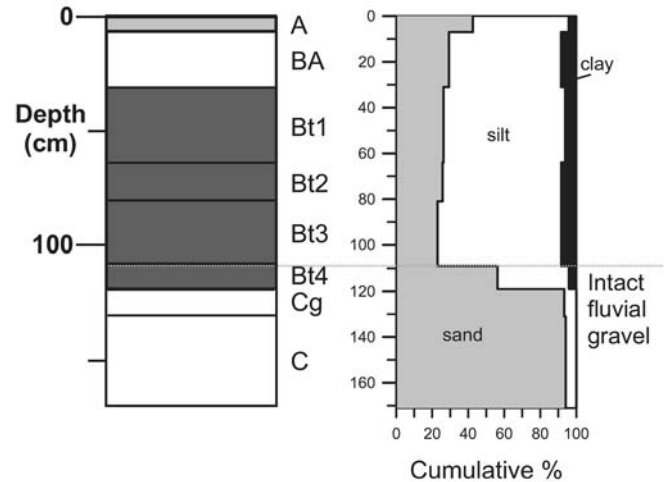


Figure 12. Soil described at Winfield gravel pit.

#### **Stop 2-4. South Fork Hoh. Twin Creeks Drift Near Confluence of South Fork Hoh and Hoh Rivers**

The purpose of this stop is to observe the well-exposed Twin Creeks drift and discuss the record of valley glaciation in the Olympic Mountains (Fig. 13). *Note: this exposure can be accessed via a similar road on the east side of the bridge, or by following the logging roads to the top of the terrace and descending the closed, terrace-edge logging road. Either access route can be rather treacherous, with the latter providing the best access to the entire exposure.* Following deposition of the Hoh Oxbow drift, the Hoh glacier retreated well upvalley, separating into two lobes at the confluence of the Hoh River and its South Fork. The two glaciers then readvanced to deposit the Twin Creeks drift. The maximum-phase Twin Creeks end moraine in the main valley lies ~2.5 km north of this exposure, adjacent the confluence area. Its South Fork counterpart lies ~3 km upvalley from this exposure, with a later-phase moraine ~2 km farther upvalley.

The stratigraphic sequence exposed here records events prior to and during the Twin Creeks 1 advance (Thackray, 2001). Three meters of grey, clast-rich till form the base of the exposure. This till correlates with the Hoh Oxbow 3 drift, the terminal moraine of which lies 12 km downvalley. Three meters of clay- and silt-rich lacustrine sediment overlie the till. Dropstones are common in the bottom meter. The lacustrine sediments yielded several wood samples, three of which yielded dates of 19,324 ± 165 (AA-18407), 19,274 ± 154 (AA-18408), and 19,169 ± 162 (AA-18406) <sup>14</sup>C yr B.P. Correlative, clast-rich glacial lacustrine sediments upvalley yielded a date on wood of 19,067 ± 329 <sup>14</sup>C yr B.P. (AA-18405). Delta sediments overlie the lacustrine beds. Ten meters of poorly exposed sand and gravel overlie the lacustrine sediments. The sediments appear to be horizontally bedded and may represent delta bottomset beds. Three meters of interbedded sand and silt with climbing ripples overlie the sand and gravel, and may also represent bottomset beds, perhaps in a

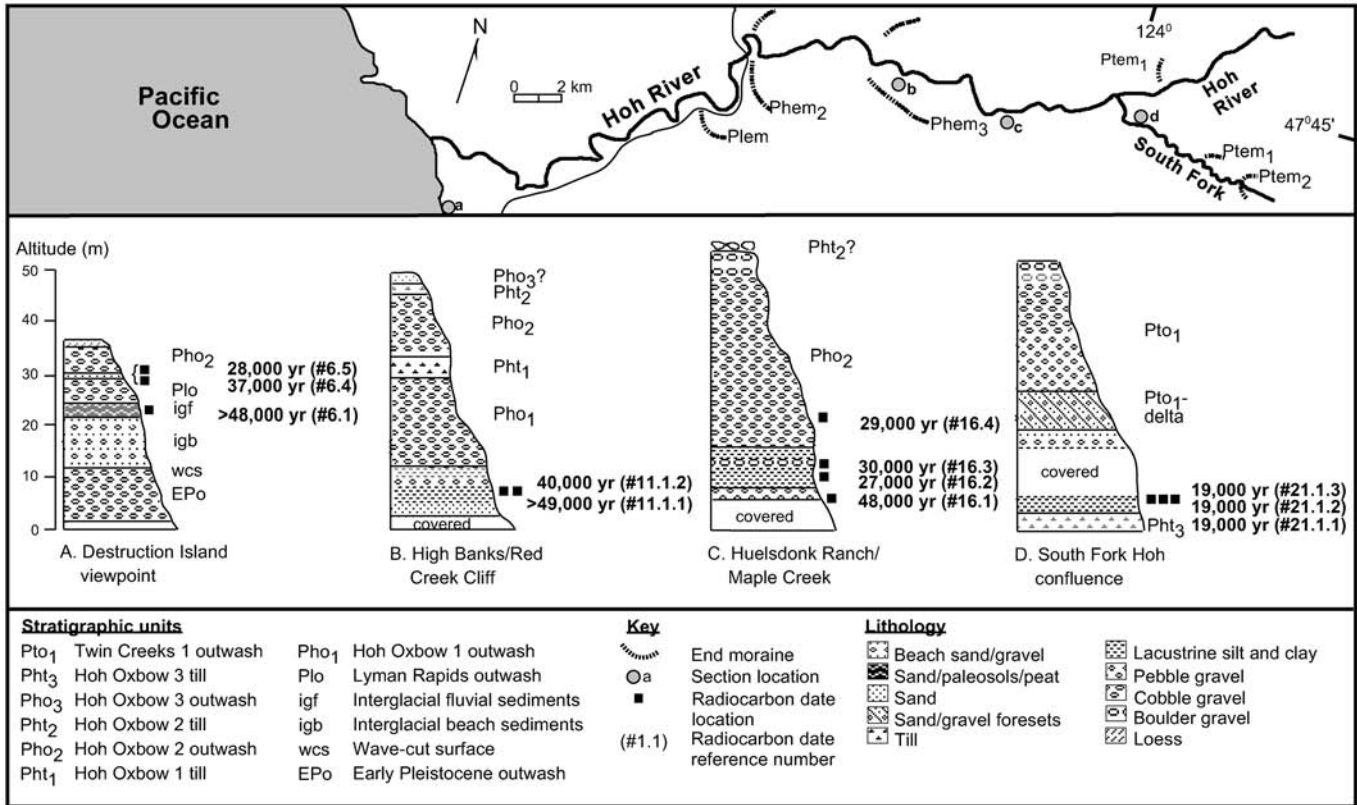


Figure 13. Correlation of glacial deposits from the coast to the field trip stop at South Fork Hoh exposures (from Thackray, 1996).

deepening lake. Northward-dipping gravel and sand delta foreset beds, 8 m thick, overlie the sand and silt. The foreset beds generally coarsen upward and are more gravel-rich in the top 2 m.

The delta sediments are overlain by ~25 m of outwash. The outwash is pebble and cobble dominated through most of its thickness, but coarsens upward to boulder-rich outwash. The top 5 m is very bouldery. The boulder-rich outwash can be observed especially well on the closed logging road ~700 m northwest of this exposure. The coarse outwash forms a prominent terrace that can be traced upvalley to the end moraine. The terrace merges with main-valley terraces in the confluence area. Till exposed in the moraine area yielded wood dated at 18,274 ± 195 <sup>14</sup>C yr B.P. (AA-16700), documenting the culmination of the Twin Creeks 1 advance at the time of the Northern Hemisphere ice-sheet maximum.

The stratigraphic sequence in this exposure reflects two advances of the South Fork glacier. The glacier first advanced past this location during the Hoh Oxbow 3 advance, depositing the till, and merged with the main Hoh glacier. It then retreated as a lake filled the valley. The valley was likely dammed by drift deposited during that advance. The lake appears to have extended into the main valley: thick sequences, clast-rich lacustrine, and deltaic sediments underlie Twin Creeks outwash on the north

side of the valley 3 km northwest of this exposure. As the South Fork glacier readvanced, an outwash delta was built into the lake. The lake was finally filled and/or the dam breached, and outwash was deposited fluviially at this location as the glacier approached its maximum position. Morphologic and stratigraphic evidence in the several kilometers upvalley of this exposure indicates that the glaciers subsequently readvanced to construct the younger Twin Creeks 2 end moraine and outwash terraces.

The Twin Creeks 1 drift was deposited at the time of the Northern Hemisphere ice-sheet maximum (ca. 18,000 <sup>14</sup>C yr B.P.). The glacier terminus was 12 km upvalley of the Hoh Oxbow 3 moraine, 17 km upvalley of the Hoh Oxbow 2 moraine (ca. 29,000–26,000 <sup>14</sup>C yr B.P.), and 20 km upvalley of the late Pleistocene-maximum Lyman Rapids moraine (55,000–130,000 yr B.P.). Thus, the alpine advance during the Last Glacial Maximum was far less extensive than advances during marine isotope stages 3 and 4. This pattern reflects the strength of westerly flow into the Olympic Mountains, which was diminished at the time of the ice-sheet maximum but sustained during earlier stadial events. The Twin Creeks 2 drift was likely deposited during the Vashon Stade (Puget Lowland maximum, ca. 14,000 <sup>14</sup>C yr B.P.), or during late-glacial time. Retrace route back to Snahapish-Clearwater Road.

Cumulative Miles (km)	Description
61.4 (99.0)	Turn left. The road follows the Snahapish Valley south into the Clearwater Valley. The Snahapish Valley occupies a low divide between the Clearwater and Hoh Valleys. The Snahapish Valley is choked with outwash and drift. At the head of the valley, this drift is mapped as Lyman Rapids (isotope stage 4). Farther downstream, as the Snahapish begins to fall into the Clearwater Valley, there is another head of outwash that we map as Whale Creek drift (isotope stage 6). We view the Snahapish Valley as being the main conduit for both water and sediment entering the Clearwater Valley at least two times in the middle and late Pleistocene.
67.5 (108.9)	Turn left on dirt road and continue into gravel pit.
67.6 (109.0)	Stop 2-5.

**Stop 2-5. Clearwater Corrections Pit**

The purpose is to examine the coarse-grained, proximal portion of the Qt2 outwash in a gravel pit adjacent to the Qt2 head of outwash. (Fig. 4). The exposures at this stop are dominated by stratified sandy gravel that is particularly coarse. Large, subangular boulders in the deposit are unique to this site and indicate that it is proximal to a head of outwash (Whale Creek, isotope stage 6). A soil was described at this site. The profile is composed of a younger, yellowish-brown late Pleistocene soil ~1 m thick that overlies reddish-brown, clay-rich horizons (Fig. 14). The base of the buried soil is not exposed. The reddish-brown buried soil is poorly preserved in only a few localities on glacial-fluvial deposits in the Hoh, Clearwater, and Queets Valleys. In most

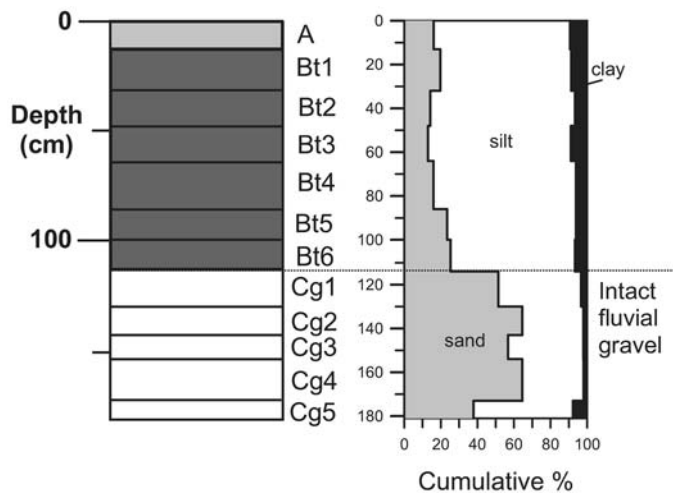


Figure 14. Soil described at the Clearwater corrections pit.

cases, the reddish-brown horizons are associated with a buried colluvial wedge; it is rarely if ever found on the deposit tread, despite the fact that the treads are typically flat. We will further develop the soil chronosequence and our interpretations of soil-landscape relationships and what they mean for landscape evolution and erosion at the stops for Day 3.

Cumulative Miles (km)	Description
67.7 (109.2)	Return to the Snahapish-Clearwater Road.
70.8 (114.2)	Turn right and follow the main, paved Snahapish-Clearwater Road through the town of Clearwater.
84.3 (135.9)	Turn right onto Highway 101 and proceed north back to Kalaloch.
94.5 (152.4)	Turn left into Kalaloch Lodge, this is the end of Day 2.

**Day 3. Clearwater Drainage, Terrace Stratigraphy, Age of Pleistocene Terraces, a Model for Holocene Terrace Genesis (Fig. 6)**

Cumulative Miles (km)	Description
0.0 (0.0)	<b>Start, Kalaloch Lodge.</b> Turn right on Highway 101 and continue on the 30 m tread.
10.2 (16.5)	Turn left on the Clearwater-Snahapish Road.
10.8 (17.4)	Cross the Queets River. The confluence of the Queets and Clearwater is ahead and to the left. Continue along the Clearwater River. As at the Highway 101 bridge, the engineering borings here demonstrate how the alluvium is thin and the stream is essentially on bedrock. The road is on a Holocene (Qt6) terrace. Older Holocene (Qt5) treads are exposed in clearcuts to the right and the treads of the two big Pleistocene fill terraces (Qt2 and Qt3) underlie the hills directly ahead.
11.5 (18.5)	Turn left onto dirt road for Clearwater Picnic bar and proceed out onto the point bar.
11.6 (18.7)	Stop 3-1.

**Stop 3-1. Clearwater Picnic Bar**

The purpose of this site is to observe the channel in the lower reaches of the Clearwater River and the stratigraphy of the river floodplain. The Clearwater River here is predominantly an alluvial stream, but the alluvium is typically less than 3 m thick. We envision most or all of this thickness of alluvium to be mobilized during large discharge events at which point it is in contact with the bedrock, driving incision. The floodplain stratigraphy is well exposed on the far bank. Depending on river stage conditions, it is possible to wade across to observe the cut bank. The cut bank exposes ~1 m of coarse sandy gravel that has a grain-size

distribution similar to the bar we are parked on. In places, the tread of this deposit is above the mean flood level. In those places, we name the tread Qt6. Here the tread continues to be inundated by floods and is named Qt7. The coarse-grained facies locally contains wood or charcoal. C-14 dates from the coarse gravelly facies 5 km upstream from this site returned an age of  $710 \pm 48$  yr B.P. Typically, this gravelly facies of Qt6 elsewhere in the watershed is dated ca. 1000 yr B.P. Stratified, locally cross-bedded sand and silt conformably overlie the gravel. The sand and silt facies is interpreted as overbank. Radiocarbon ages range from modern to several centuries before present and the virtual lack of any soil development attest to the continued aggradation of this unit. The Holocene terrace visible at this location is just one of several Holocene and late Pleistocene terraces that will be seen at the next stops (Fig. 15).

Return to the Snahapish-Clearwater Road.

Cumulative Miles (km)	Description
11.7 (18.9)	Turn left.
14.4 (23.2)	Begin ascent of the Qt3 terrace.
14.9 (24.0)	To the left and down the bank is a 30 m high landslide headwall exposure of Qt3 gravels

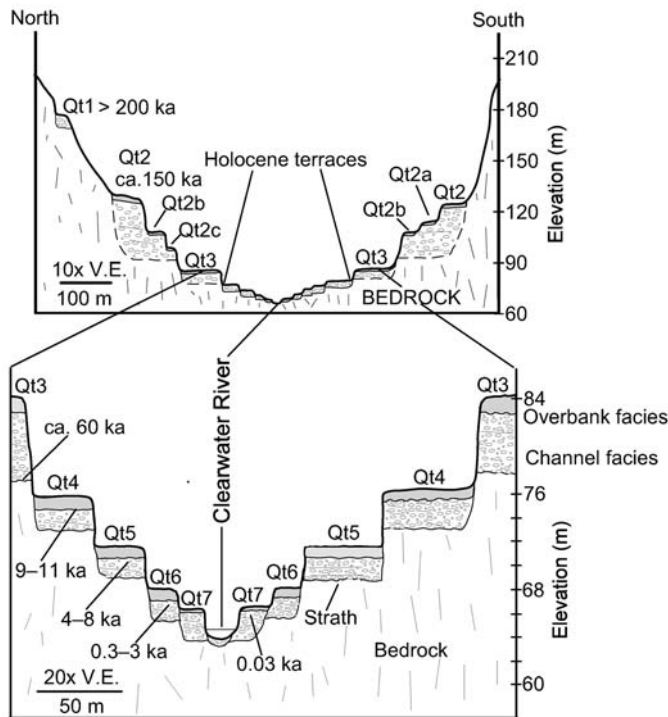


Figure 15. Composite cross section representing the terrace stratigraphy and general age ranges in the Clearwater drainage. We use the convention of naming terraces in order of increasing age where 1 is the oldest (highest) terrace in the landscape and assigning numbers to straths only. In this manner, terrace Qt2 may have more than one tread, which we designate with lower case alpha numeric subscripts (as Qt2a, Qt2b).

unconformably overlying lacustrine beds. The lacustrine beds have been dated at  $>47,000$  radiocarbon yr B.P. and are likely correlative to Qt2. The overlying Qt3 alluvium has a reported finite age of  $48,300 \pm 3,300$  radiocarbon yr B.P. (Thackray, 1996; likely also an infinite age).

- 16.4 (26.5) Rise onto a degraded tread of Qt2 ~20 m above the Qt3 tread.
- 18.0 (29.0) Cross Elkhorn Creek incised into the alluvium of Qt3. Slow for a left turn.
- 18.1 (29.2) Turn left onto dirt road and park.

**Stop 3-2. Qt3 at the Elkhorn Pit**

The purpose of this stop is to show the sedimentology, stratigraphy, and weathering characteristics of the Qt3 terrace and to develop arguments that the underlying strath was buried at 60 ka, and the Qt3 terrace deposit and tread are correlative to the 30 m coastal terrace. Qt3 has a moderately developed yellow soil profile (Fig. 16) and an oxidation depth of 4–5 m, but locally 10 m in coarse alluvium. Post-depositional modification is minimal on the terrace treads, which retain a constructional morphology with well-preserved sandy overbank and silty loess deposits. The loess is more than 1 m near the Snahapish River and near the coast. Soil profiles consist of a 50–80-cm-thick B horizon composed of yellowish-brown (10YR) to brown (10YR–7.5YR) silt loam with numerous thin clay films preserved on soil ped faces. Soil profiles in fine-grained material have strong brown colors (7.5YR) and well-developed soil structure. Qt3 is best preserved below approximately km 24, where it locally has two treads, designated as Qt3a and Qt3b, with the Qt3b tread sitting ~4 m below the Qt3a tread. In this part of the valley, Qt3 straths maintain a gentle gradient, lying 6–10 m above the channel, and treads are 35 m above the channel. Above km 24, Qt3 has only one tread, and the straths take on a

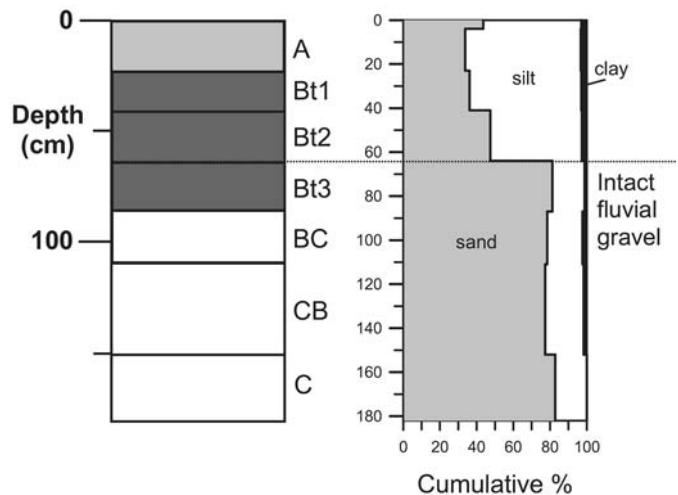


Figure 16. Soil described at Elkhorn Creek.

steeper gradient, climbing to a maximum height of 70 m above the channel. This gravel-pit outcrop of Qt3 exposes a highwall cut into the Qt3b tread. The Qt3 tread can be traced upstream through the Snahapish Valley to the Lyman Rapids (isotope stage 4, ca. 60 ka) head of outwash in the Hoh Valley (Fig. 3).

Return to vehicles and return to the Clearwater-Snahapish Road. Turn left.

Cumulative Miles	(km)	Description
18.2	(29.4)	Cross Shale Creek.
18.3	(29.5)	Stay left on the paved main road.
19.2	(31.0)	Slow and pull off the road to the left in the parking area just before the bridge. The outcrop is a short walk down the dirt road leading to the river. Stop 3-3.

**Stop 3-3. Holocene Strath at the Grouse Bridge**

The purpose of this stop is to introduce the concept of a strath, the terrace deposit, and some of the relative and numeric criteria in establishing strath age. Detailed discussions of these topics can be found in Wegmann (1999), Pazzaglia and Brandon (2001), and Wegmann and Pazzaglia (2002). Terraces are well preserved in the Clearwater drainage. There are two major flights of terraces: a higher, outer, older sequence that is underlain by thick alluvial-fill deposits, and a lower, inner, younger sequence underlain by thin alluvial deposits (Fig. 15). The terrace exposed here at the Grouse Bridge is a fine example of the lower, inner, younger sequence, and it contains all of the stratigraphic characteristics important to distinguishing and using terraces in tectonic interpretations (Figs. 17 and 18). The lower terraces like the one exposed here are composed of a basal, coarse-grained, 1–3-m-thick axial channel, sandy gravel facies, and overlying fine-grained 1–3-m-thick sandy silt overbank facies. The sandy gravel facies locally preserve sedimentary structures consistent with lateral accretion processes, as might be expected for point and transverse bars, which can be seen in the adjacent modern channel. So by analogy, we take the coarse-grained facies of the terrace deposit to represent the bedload being transported when the terrace strath was cut. In contrast, the fine-grained facies represent vertical accretion atop the floodplain, presumably related to deposition during floods.

Return to vehicles and continue across the Grouse Bridge on the Snahapish-Clearwater Road.

Cumulative Miles	(km)	Description
19.9	(32.1)	Cross the Clearwater River and ascend the Qt3 tread. As the road continues to climb, bedrock is exposed in the valley wall.
20.8	(33.5)	Cross Christmas Creek. Like the Snahapish River, alluvium from the Hoh River spilled into the Clearwater drainage through this valley.
21.2	(34.2)	Climb out of the Christmas Creek Valley and ascend onto the Qt2 tread.

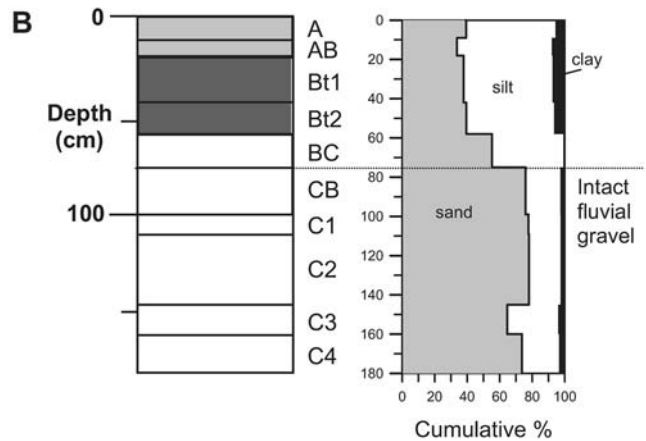


Figure 17. A: Annotated photograph of the Qt5 strath and strath terrace exposed at the Grouse Bridge. B: Soil described at the Grouse Bridge site in Qt5.

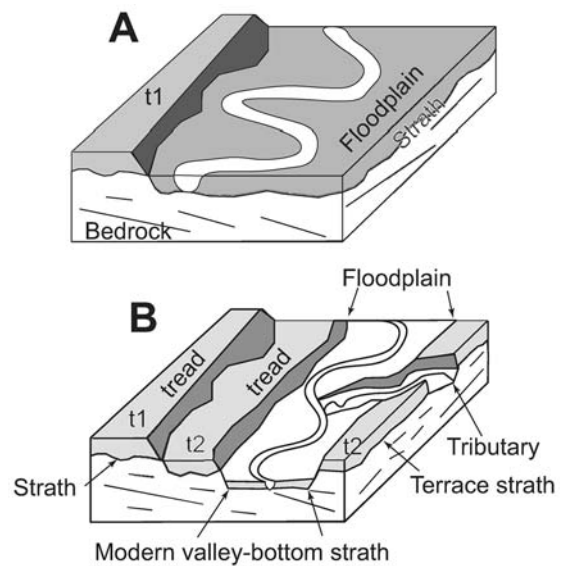


Figure 18. A: Schematic illustrating the relationship between a terrace (t1, t2), straths, the floodplain, and a valley bottom. B: The correspondence between the width of the floodplain and the width of the valley bottom strath is corroborated by exposure of the valley bottom strath in tributary channels, shown entering from the right part of the diagram.

- 22.0 (35.5) Continue along a long, flat portion of the Qt2 tread.
- 22.8 (36.8) Begin descending the Qt2 tread and stay right onto the dirt road leading to the Coppermine Bottom campground.
- 22.9 (36.9) Proceed straight down to the campground. Descend Qt2, cross Crooks Creek slough, and a fill unit inset into the Qt3 tread.
- 23.5 (37.9) Traverse the Qt3 tread and turn right.
- 24.0 (38.7) Stop 3-4.

**Stop 3-4 and Lunch. Coppermine Bottom**

The purpose of this stop is to observe a reach of the Clearwater River channel near the middle part of the watershed and discuss the observed and modeled distribution and rates of incision of the Clearwater channel. Tomkin et al. (2003) uses the incision data for the Clearwater River to test a variety of models for incision of bedrock channels. We refer you there for details of this analysis. Figure 19 provides a simple summary of the main results. Models like the unit-shear stress model or stream-power model for incision assume a functional form of  $I = kS^nQ_p^m$ , where  $I$  is the long-term incision rate,  $S$  is the gradient of the channel, and  $Q$  is the discharge normalized for channel width. The parameters  $k$ ,  $n$ , and  $m$  have different predicted values, depending on the model, but all models require that  $n$  and  $m$  are greater than zero. Figure 19 shows the best-fit solution for the model equation given. The transformation to logarithms allows the equation to be fitted by a plane, as indicated by  $I = \ln k + n \ln S + m \ln Q_p$ . The best-fit solution is shown in Figure 19. What should be obvious is that the slope of the plane is negative for both  $\ln S$  and  $\ln Q_p$ , which means that the predicted values for  $m$  and  $n$  are less than zero. Thus, available models do not adequately fit the data for the Clearwater. We will summarize possible solutions for this paradox.

After lunch, loop through the campground and retrace route out to the Clearwater-Snahapish Road.

Cumulative Miles (km)	Description
25.6 (41.3)	Stay left and then make a quick right into the Copper Pit (gravel pit).

**Stop 3-5. Qt2 Terrace at the Copper Pit and Cosmogenic Surface Dating Profile**

The purpose of this stop is to show the sedimentology, stratigraphy, and weathering characteristics of the Qt2 terrace and develop the arguments that the underlying strath is 150 ka, whereas the terrace deposit and tread are correlative to the 60 m coastal terrace. Cosmogenic results should be available at the time of the field trip. Qt2 is the thickest and most widespread fill terrace in the Clearwater Valley. Qt2 terrace deposits are made up of 5–40 m of coarse stratified sand and gravel that sit on straths 0–20 m above the level of the modern valley bottom (Figs. 13 and 20). Locally, the fill has buried not only the paleovalley bottom (equivalent to the strath) but also the side slopes of the river

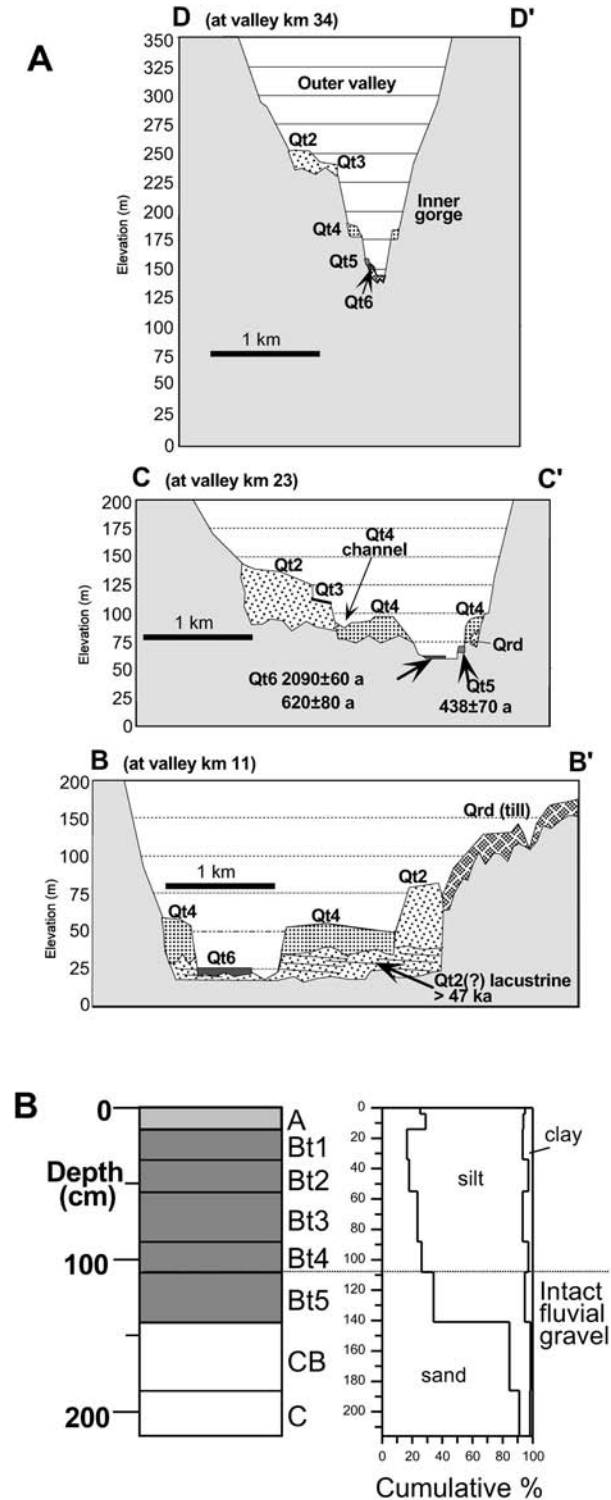


Figure 19. Best-fit solution for the Clearwater River incision data, assuming a stream-power type function. Dark circles are the Qt2 strath (ca. 140 ka) and open circles are the Qt3 strath (ca. 65 ka).  $I_{rate}$  is the incision rate,  $S$  is the channel gradient, and  $Q_p$  is the modern average discharge normalized for channel width. Each of these variables is plotted on logarithmic axes. The slope of the best-fit plane indicates that the parameters  $m$  and  $n$  are less than zero, which is not permitted by stream power model. See text for further discussion and also Tomkin et al. (2003).

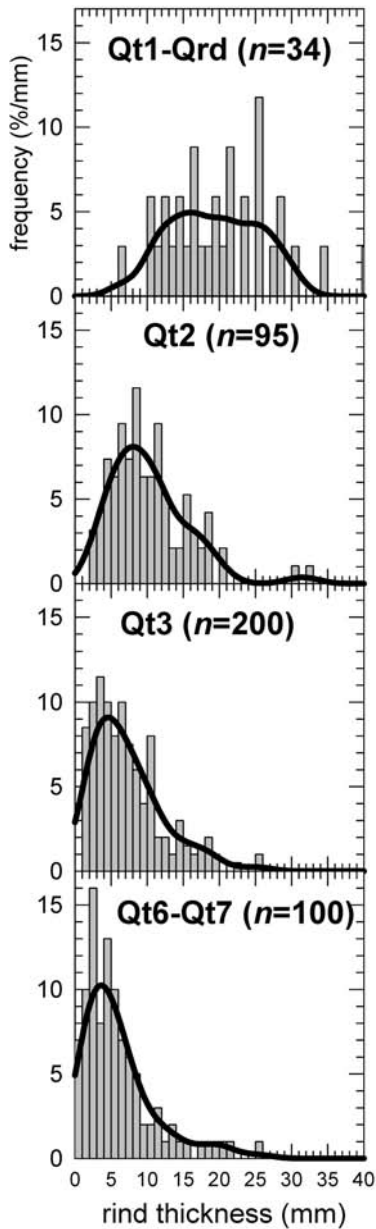


Figure 20. A: Cross-valley profiles of the lower (B–B'), middle (C–C'), and upper (D–D') parts of the Clearwater Valley showing the relationship of the terrace units to the local valley geometry. Locations are shown in Figure 4A. B: Soil described in road cut, 100 m west of Copper Pit. V.E.—vertical exaggeration.

valley itself, thus forming a buttress unconformity. Sedimentary structures within the terrace deposits include broad, shallow channel forms exhibiting 0.5–2-m-high tabular crossbeds and smaller-scale trough crossbeds of silty sand. These sedimentary structures are generally consistent with a braided channel form and mimic the features exhibited by glaciofluvial deposits that can be physically traced to heads of outwash in adjacent, glaciated drainages. The terrace alluvium is capped by ~1–2 m of

thin-bedded sand, locally laminated silt, and massive silt, which are interpreted as both overbank and loess deposits.

Soil profile development and clast weathering rinds (Figs. 20 and 21) in the terrace treads allow distinctions between deposits of different age and correlation between upstream and downstream remnants of the terraces. The Qt2 terrace alluvium represents a time of major Clearwater Valley aggradation, when the middle and lower portion of the drainage were hydrologically connected to the Hoh drainage (Fig. 4). Downstream, the Qt2 tread can be traced nearly unbroken to the 60 m coastal terrace, which we have already argued was likely deposited during isotope stage 6 or ca. 150 ka. So here, we have the upstream projection of that isotope stage 6 fill to its head of outwash in the Snahapish Valley. The timing of aggradation must be limited upstream by when the ice margin was stalled in the Snahapish Valley pumping out sediment and discharge, and downstream by when sea level was rising to produce the accommodation space leading to the high elevation of the Qt2 tread. This restricts the filling to between 150 and 125 ka. So the strath at the base of Qt2 is taken as 150 ka, and the tread is considered to be younger (Fig. 7).

Return to Snahapish-Clearwater Road, turn right and retrace route back to Grouse Bridge.

	<i>Cumulative</i>		
	<i>Miles</i>	<i>(km)</i>	<i>Description</i>
29.2	(47.1)		Cross Grouse Bridge.
30.0	(48.4)		Turn left onto the C1000 road. This road will ascend the Qt3 tread, here ~30 m above the valley bottom.
31.3	(50.5)		Ascend the degraded remnants of the Qt2 tread.
31.8	(51.3)		Stay right on the major C1000 road. The dirt road leading off to the left is the old approach to the former Goodyear Bridge, an old suspension bridge no longer suitable for vehicle traffic. C1000 continues to follow the Qt3 tread.
33.6	(54.2)		Cross Deception Creek and then begin ascending the bedrock ridge north of the Deception Creek drainage.
34.0	(54.8)		Find a safe place to park. You may have to take advantage of the C1200–C1000 road intersection 0.5 mile farther up the road. This is where we need to descend the bank down to the Clearwater River. At the river, find a gravel bar and follow it onto the big north-facing meander loop. Stop 3-6.

### Stop 3-6. Crooks Creek Terraces

The objective here is to use the view to illustrate the magnitude of strath separation and resulting river incision rates. The maps and ages of Pleistocene and Holocene terraces will be used to develop models of terrace formation influenced by climatic and tectonic forcing (Meyer et al., 1995; Pazzaglia and Brandon, 2001; Wegmann and Pazzaglia, 2002; Figs. 22, 23, 24, 25, and 26).

Retrace route out the C1000 road.

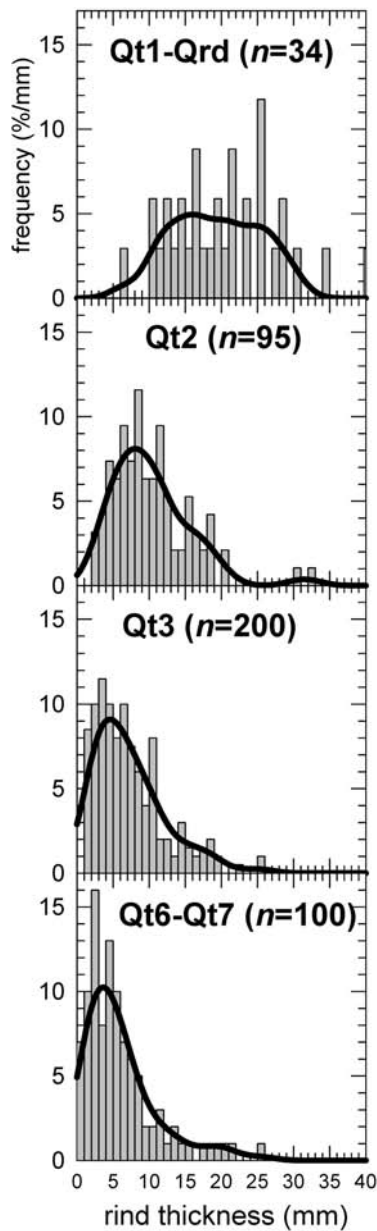


Figure 21. Thickness distributions for clast weathering rinds for terrace deposits of different stratigraphic age. The probability density curves were calculated using the Gaussian kernel method (Brandon, 1996), with the kernel size set to 2 mm. Qt1-Qrd is from an interfluvium ~180 m elevation on the north divide of Shale Creek. Qt2 is from the Peterson Creek terrace ~130 m elevation. Qt3 is from the Quinault quarry pit ~30 m elevation. Qt6 is from an exposed gravel bar adjacent to the Clearwater River, near the Clearwater Picnic Area, ~2 km south of the town of Clearwater.

Cumulative		Description
Miles	(km)	
38.0	(61.3)	Proceed straight on the Snahapish-Clearwater Road, turn right on Highway 101 and return to Kalaloch.

**Optional stops for Day 3**, weather and interest permitting. Both routes are logged from the intersection of the Coppermine Bottom access road and the Snahapish-Clearwater Road.

**Optional Log 3-A. Upper Basin and Terraces at Kunamakst Creek**

Cumulative		Description
Miles	(km)	
0.0	(0.0)	Turn right onto the Snahapish-Clearwater Road.
0.5	(0.8)	Turn right directly before the Snahapish River Bridge (on the Clearwater-Snahapish Road) and begin driving up the Snahapish Valley.
4.5	(7.3)	Turn right at the major triangle intersection onto the C2000 road.
7.3	(11.8)	Loop around steep tributaries. The Qt2 tread is visible in the clearcuts on the right.
8.6	(13.9)	Slow and turn right into dirt road marked W-5 or C2017. Pull forward and park to the left in the opening.
8.7	(14.0)	Walk south on the overgrown dirt road leading out to an old clearcut.

**Optional Stop 3-A. Terraces at Kunamakst Creek**

This is an overview stop to illustrate the presence of terraces, straths, and their considerable separation from the modern channel in the upper Clearwater drainage.

Return to vehicles and retrace route out to the triangle intersection with the Clearwater-Snahapish Road, stay left back toward Coppermine Bottom.

**Optional Log 3-B. Grouse Creek Landslide**

Cumulative		Description
Miles	(km)	
0.0	(0.0)	Turn right onto the Snahapish-Clearwater Road.
0.5	(0.8)	Cross the Snahapish River and stay to the right on the paved road (toward Upper Clearwater campground).
1.4	(2.3)	Here, and at several other places, you will pass exposed gravels of the Qt2 terrace.
2.5	(4.0)	Cross the Qt2 tread.
3.9	(6.3)	Cross the Clearwater River at the Upper Clearwater campground. Qt5 terraces, like the one observed at the Grouse Bridge, are exposed both upstream and downstream of the bridge on the bank straight ahead.
4.5	(7.3)	Stay right on the C3100 road. Begin traversing the interfluvium between the Solleks River and

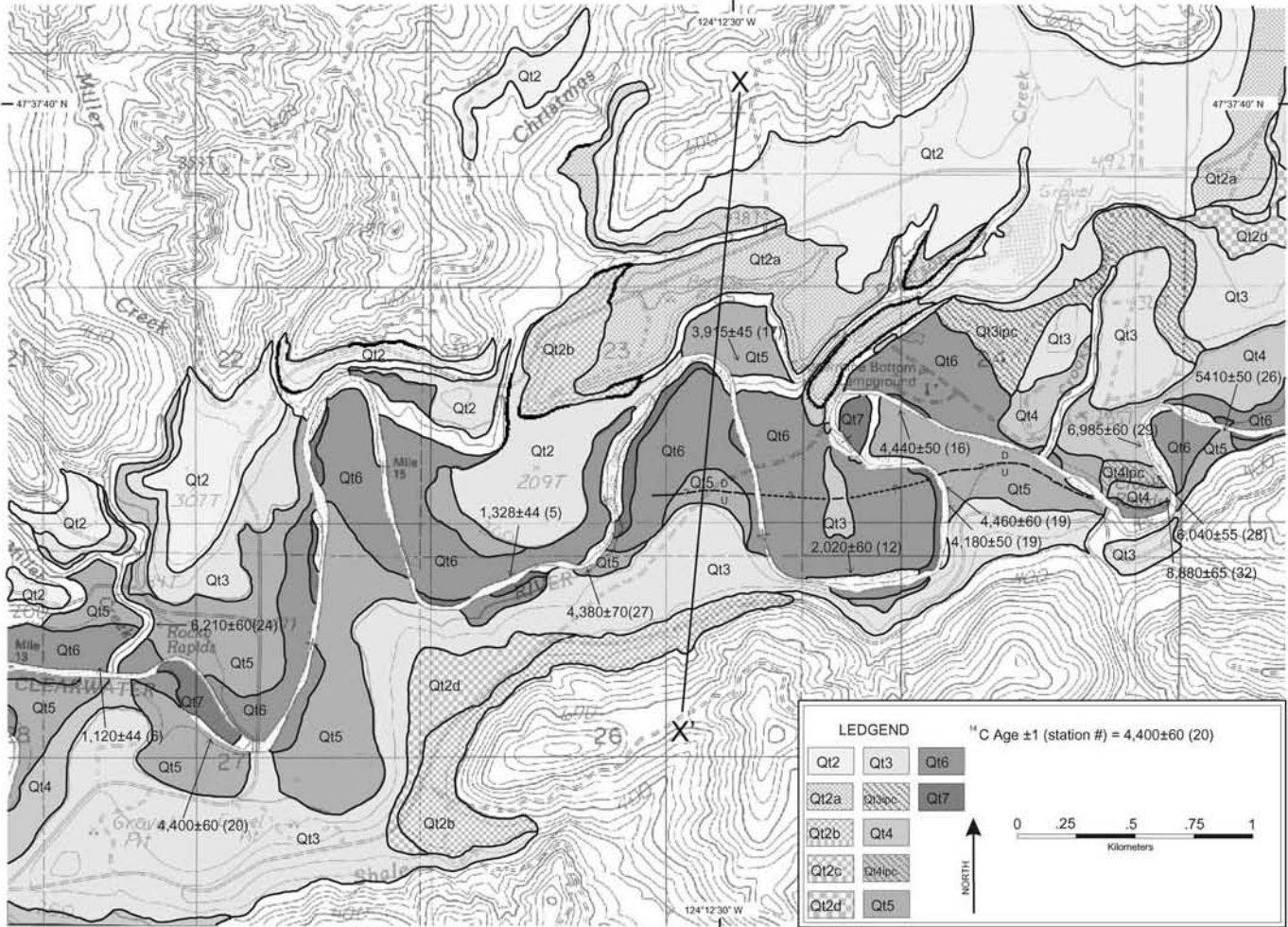


Figure 22. Map of river terraces in the medial portion of the Clearwater Valley (modified from Wegmann, 1999). Letters following terrace-name designations: a, b, c, d indicate trends that share a common strath; ipc indicates inset paleochannel.

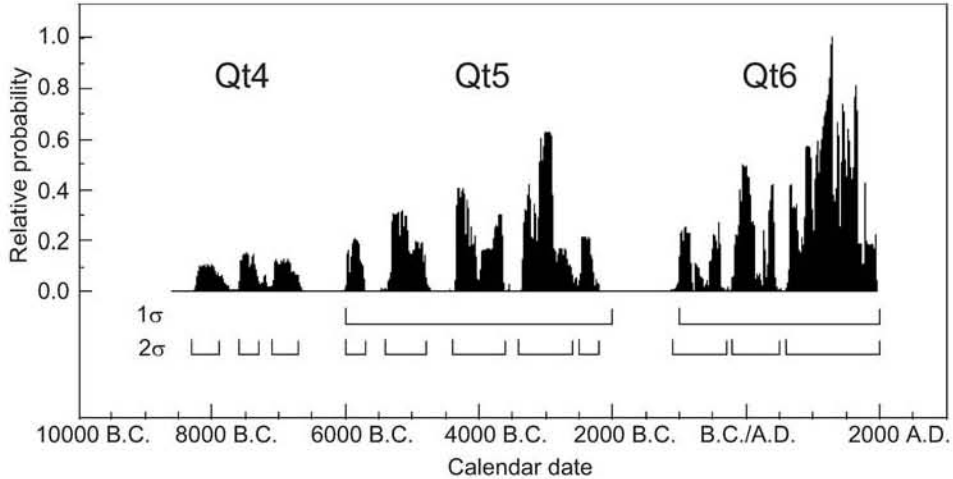


Figure 23. Probability density and frequency plots for 38 radiocarbon dates of the Holocene terraces. The plot was produced by calculating calendar ages, their accompanying  $1\sigma$  errors, and then summing the probabilities using the program OxCal (Ramsay, 2000). Note the brackets beneath the frequency histograms. At the  $1\sigma$  confidence level, the group of ages between 6000 and 2000 B.C. and 1000 B.C. and 2000 A.D. statistically coincide with terraces Qt5 and Qt6, respectively.

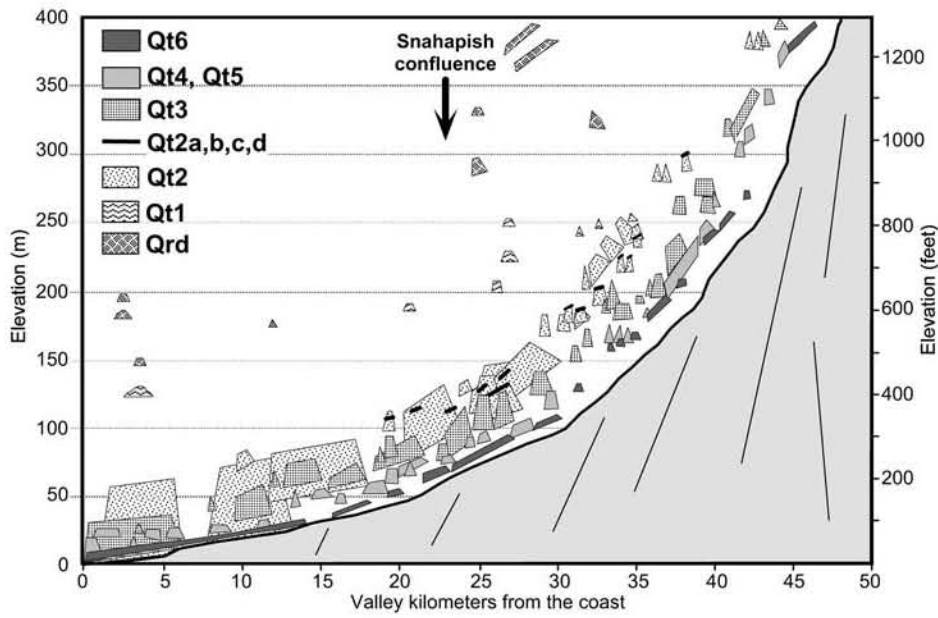


Figure 24. A long-profile section of the Clearwater Valley showing the vertical relationship of mapped terrace deposits (polygons) to the modern Clearwater River (continuous line). Terrace units were projected orthogonally into the valley profile from their mapped positions along the flanks of the Clearwater Valley (Fig. 4B). The bottom and top of each polygon corresponds to the strath and tread, respectively, for a mapped terrace deposit.

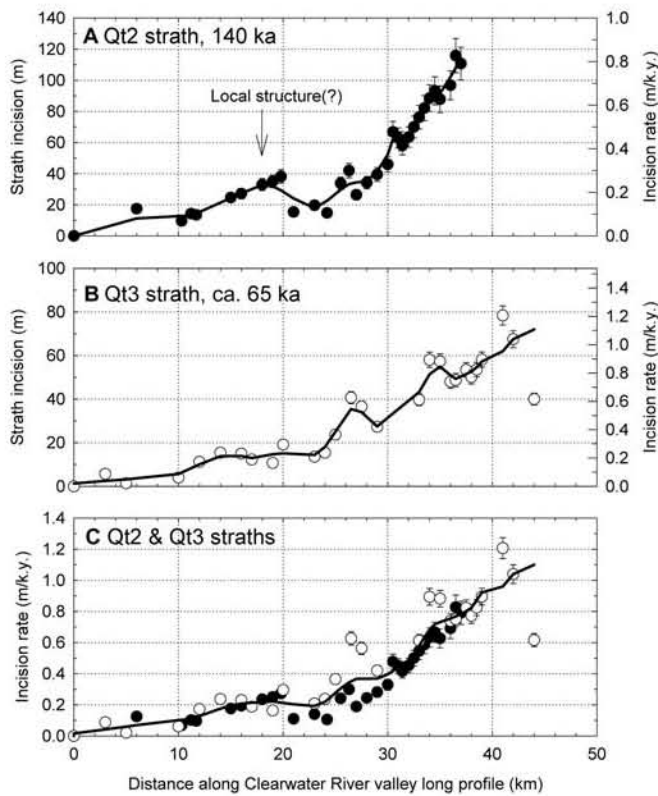


Figure 25. Incision of the (A) Qt2 and (B) Qt3 straths with respect to distance along the valley long profile (see Fig. 4B). C: Incision rates calculated from the Qt2 strath (solid circles) and Qt3 strath (open circles). Note the similarity in the estimated long-term incision rates for these two different-age straths. In general, incision and incision rates increase in an upstream direction. The small bump in the profiles at ~15–25 km suggests some localized uplift, such as a broad fold. Error bars show  $\pm 2$  standard error uncertainties due to measurement errors for strath height. The thick lines are smoothed from the original data using a locally weighted regression method (Lowess algorithm of Cleveland, 1979, 1981, with the interval parameter set to 0.2).

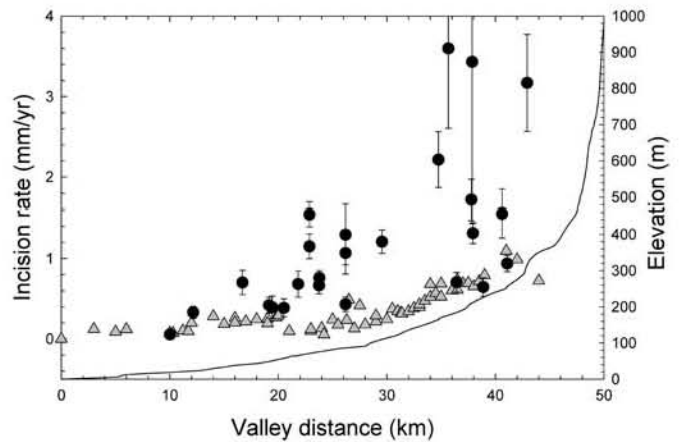


Figure 26. Incision rates (left vertical axis) for the Clearwater Basin determined from Holocene terraces (solid black circles) and Pleistocene terraces (gray triangles) plotted with respect to distance along the valley long profile (right vertical axis). Rates reflect calendar ages and error bars on the Holocene data are  $1\sigma$  standard error. Note that the incision rates for both data sets increase upstream.

- 6.2 (10.0) Stequaleho Creek, both major tributaries to the Clearwater River. Turn left onto the C3140 road. Note that this road is gated by the Washington Department of Natural Resources just past the junction with the C3100 road. Vehicle traffic past this gate is allowed by permission of the department. To obtain permission and a key to the gate, contact the Olympic region office in Forks (360-374-6131). Foot and bike access is allowed without permission.
- 7.7 (12.4) Stay on the main road.
- 10.0 (16.1) Drop into the Solleks Valley bottom.
- 11.6 (18.7) Cross the Solleks River.
- 12.1 (19.5) To the south across the old gravel pit is an unobstructed view into the Grouse Creek drainage and the 1997 landslide.
- 13.0 (21.0) Turn right onto the C3185 road. Cross the Solleks River again and begin ascending the ridge on the south side of the river.
- 14.0 (22.6) Negotiate switchbacks.
- 15.1 (24.4) Stay to the right, turning onto the C3100 road.
- 15.5 (25.0) Stay to the right (straight on C3100 road).
- 15.7 (25.3) Park vehicles near the short access roads connected to the main dirt road. Stop 3-7.

**Stop 3-7. Grouse Creek Landslide**

The objective here is to illustrate the magnitude of mass wastage and sediment delivery to the channel occurring during the Holocene. *Note: Due to road deconstruction, one has to walk ~1 km to the headscarp of the landslide on the unmaintained road.* On March 19th, 1997, 506,000 m<sup>3</sup> of rock and regolith moved off this hillslope and into the Solleks River (Serdar, 1999; Gerstel, 1999). The landslide occurred during the waning phases of a major rain-on-snow flood event that started two days prior on March 17th (the St. Patrick's Day flood). Approximately 200,000 m<sup>3</sup> of material was deposited on the upper slopes of the Grouse Creek channel, with the remainder moving as a debris flow that traveled down Grouse Creek, picking up additional material from side slopes, which were scoured up to 54 m high. When the debris flow reached the Solleks River, it deposited ~78,000 m<sup>3</sup> of material. Landsliding here may have been exacerbated by both a road and associated logging activity; earlier slide scars and additional landslides cut adjacent hillslopes.

The debris delivered to the Solleks channel temporarily dammed the river and pushed the channel to the north. A plume of coarse sediment worked its way down the Solleks into the Clearwater channel by the summer of 1997. The net effect of such instantaneous, point introductions of sediment was to force the channel to enhance its lateral corrasion as the sediment was temporarily stored in floodplains and in channel bars. Downed trees recruited from floodplains trapped the sediment and locally made alluvial fills behind dams of woody debris. The abundance of woody debris dams increased in frequency

on the Clearwater River in the reach directly downstream of the Solleks confluence.

Return to vehicles and retrace route all the way back to the Upper Clearwater campground and then on the paved road back to the Snahapish River bridge.

**Day 4. Kalaloch to Queets River, Lake Quinault, Hoquium, Seattle**

<i>Cumulative</i>		<i>Description</i>
<i>Miles</i>	<i>(km)</i>	
0.0	(0.0)	Depart Kalaloch Lodge, turn right onto U.S. Rt. 101 south.
12.0	(19.4)	Turn left, entrance to Queets River valley.
24.0	(38.7)	Stop 4-1.

**Stop 4-1. Queets River Valley**

The purpose of this stop is to discuss cosmogenic erosion rates based on cosmogenic inventories of channel alluvium. Return to U.S. Rt. 101.

<i>Cumulative</i>		<i>Description</i>
<i>Miles</i>	<i>(km)</i>	
36.0	(58.1)	Turn right onto U.S. Rt. 101.
53.5	(86.3)	Stop 4-2.

**Stop 4-2. Lake Quinault**

The purpose of this stop is to observe the Hurricane Ridge fault as well as the glacially dammed Lake Quinault. The Hurricane Ridge fault at this location is steeply dipping and juxtaposes the Crescent Formation against the Hoh Formation, which is largely buried by glaciofluvial deposits along the southeast flank of the Quinault Valley. Lake Quinault is dammed by late Pleistocene, presumably Hoh Oxbow-equivalent moraines.

Continue south on U.S. Rt. 101.

<i>Cumulative</i>		<i>Description</i>
<i>Miles</i>	<i>(km)</i>	
94.0	(151.6)	Stop 4-3.

**Stop 4-3. Hoquium**

The purpose of this stop is to observe a cut-bank exposure where a buried marsh marking rapid coastal emergence during the 1700 A.D. earthquake is exposed.

**CONCLUDING REMARKS**

Our study uses fluvial geomorphology and Quaternary stratigraphy to reconstruct the Quaternary landscape evolution and rock uplift across the Olympic sector of the Cascadia subduction zone. Glacial deposits and a well-preserved terrace stratigraphy in an unglaciated drainage allow us to use coastal exposures and the valley profile of the Clearwater as a crude geodetic datum. As

such, we are able to quantify the effects of both the short-term earthquake cycle and permanent wedge deformation driving uplift across the interior of the Olympic Peninsula.

1. Uplift and formation of Olympic topography is primarily a result of northeast-directed shortening parallel to the direction of plate subduction. Thermochronology and other erosion rate data support removal of at least 12 km of rock from the Olympic Mountains core at a current modern rate of  $\sim 1$  mm/yr. These results do not discredit the data which suggests north-south shortening along the Coast Ranges, but the north-south shortening simply cannot account for the degree of shortening and removal of rock that has been accomplished by growth and deformation of the Olympic accretionary wedge.

2. A buried sea cliff, probably formed at 122 ka, provides evidence of horizontal motion of rock relative to the modern shoreline. The rate of motion is 3.7 m/k.y. to the northeast, which is close to the 3 m/k.y. horizontal material velocity predicted for a frontally accreting steady-state wedge. These results are consistent with a kinematic model in which long-term horizontal velocity may account for 20%–35% of the geodetically measured horizontal velocity across the Olympics (Pazzaglia and Brandon, 2001). The remaining 65%–80% is presumably elastic deformation.

3. There are five recognized periods of alpine glaciation for the western Olympic Peninsula. The relative extent of these glaciations reflects a complex interaction between temperature and available moisture, controlling the equilibrium line altitude (ELA). The extent of alpine ice was limited when the Cordilleran Ice Sheet was farthest south, presumably because storm tracks bringing moisture to western North America were depressed southward.

4. Pleistocene terrace sequences in the Olympics seem to be closely tied to the glacial climate cycle through its influence on local climate, sediment supply from adjacent alpine-glaciated drainages, and eustasy. The sequence of terrace-forming events is consistent with the model of Bull (1991), but the timing of these events relative to the eustatic cycle is quite different. Bull (1991) proposed that strath formation occurred during rising sea level and aggradation during falling sea level. In the Olympics, strath formation seems to occur during peak glaciation (when sea level is low), and aggradation during late glacial and interglacial times, when sea level is rising. We suspect that this difference is a local effect, related to the strong influence that local deglaciation has had on sediment supply and the interaction of that enhanced sediment supply with rising sea level during interglacial times.

5. Holocene terraces represent local-scale processes of enhanced lateral incision, valley-bottom widening, and the carving of straths accomplished with the aid of the thin alluvial deposits preserved atop the straths. Valley bottom narrowing and rapid vertical incision into bedrock is accomplished during relatively brief (1000 yr) intervals between the carving of the major straths.

6. The upstream divergence of straths in the Clearwater drainages provides strong evidence that uplift is very slow at the coast and increases to a maximum in the center of the range. This conclusion runs counter to a commonly invoked assumption in fluvial geomorphology that long-term uplift rates can be taken as

uniform within a single drainage. The incision rates correspond closely with the pattern of long-term erosion rates indicated by apatite fission-track cooling ages. These observations indicate that, at long time scales (10–100 k.y.), the average form of the landscape remains close to steady state. This also implies that during each phase of strath cutting, the Clearwater Valley profile is able to return to the same steady-state form. Thus, bedrock incision rates seem to be a reasonable proxy for rock uplift rates in the Olympics.

7. The profile of incision and erosion rates across the Olympics indicates a close balance between the accretionary and erosional fluxes moving in and out of the wedge. This result supports the hypothesis of Brandon et al. (1998) that the Olympic sector of the Cascadia wedge is close to a flux steady state, but note that this conclusion does not require the topography to be steady as well.

## ACKNOWLEDGMENTS

The authors would like to acknowledge long-standing working relationships with geoscientists that have worked with us, supported us, and inspired discussion on the topics presented in this paper. These include, but are not limited to Bill Lingley, Wendy Gerstel, Sean Willett, Joe Vance, Tony Garcia, John Garver, Mary Roden-Tice, and Brian Atwater. We thank the Quinault Nation, State of Washington, Olympic National Park, and Rayonier Inc. for access to their respective lands. Research supported by National Science Foundation grants EAR-8707442, -9302661, -9405659, and -9736748.

## REFERENCES CITED

- Adams, J., 1984, Active deformation of the Pacific Northwest continental margin: *Tectonics*, v. 3, p. 449–472.
- Ahnert, F., 1970, Functional relationships between denudation, relief, and uplift in large mid-latitude drainage basins: *American Journal of Science*, v. 268, p. 243–263.
- Armentrout, J.M., 1981, Correlation and ages of Cenozoic chronostratigraphic units in Oregon and Washington, *in* Armentrout, J.M., ed., *Pacific Northwest Cenozoic biostratigraphy*: Geological Society of America Special Paper 184, p. 137–148.
- Atwater, B., 1996, Coastal evidence for great earthquakes in western Washington, *in* Rogers, A.M., Walsh, T.J., Kockelman, W.J., and Priest, G.R., eds., *Assessing earthquake hazards and reducing risk in the Pacific Northwest; Volume 1: U.S. Geological Survey Professional Paper 1560*: Reston, Virginia, U.S. Geological Survey, p. 77–90.
- Atwater, B.F., 1987, Evidence for great Holocene earthquakes along the outer coast of Washington State: *Science*, v. 236, p. 942–944.
- Atwater, B.F., Stuiver, M., and Yamaguchi, D.K., 1991, Radiocarbon test of earthquake magnitude at the Cascadia subduction zone: *Nature*, v. 353, p. 156–158.
- Batt, G.E., Brandon, M.T., Farley, K.A., Roden-Tice, M., 2001, Tectonic synthesis of the Olympic Mountains segment of the Cascadia wedge, using two-dimensional thermal and kinematic modeling of thermochronological ages: *Journal of Geophysical Research*, v. 106, no. B11, p. 26,731–26,746.
- Baumont, C., Ellis, S., and Pfiffner, A., 1999, Dynamics of subduction-accretion at convergent margins: Short-term modes, long-term deformation, and tectonic implications: *Journal of Geophysical Research*, v. 104, p. 17,573–17,602.
- Beck, M.E., Jr., and Engebretson, D.C., 1982, Paleomagnetism of small basalt exposures in the West Puget Sound area, Washington, and speculations on the accretionary origins of the Olympic Mountains: *Journal of Geophysical Research*, v. 87, p. 3755–3760.

- Bigelow, P.K., 1987, The petrology, stratigraphy and drainage history of the Montesano Formation, southwestern Washington and southern Olympic Peninsula [M.S. Thesis]: Bellingham, Washington, Western Washington University, 263 p.
- Bockheim, J.G., Kelsey, H.M., and Marshall, J.G., III., 1992, Soil development, relative dating, and correlation of late Quaternary marine terraces in southwestern Oregon: *Quaternary Research*, v. 37, p. 60–74.
- Brandon, M.T., 1996, Probability density plots for fission-track grain age distributions: *Radiation Measurements*, v. 26, p. 663–676.
- Brandon, M.T., and Calderwood, A.R., 1990, High-pressure metamorphism and uplift of the Olympic subduction complex: *Geology*, v. 18, p. 1252–1255.
- Brandon, M.T., and Vance, J.A., 1992, Tectonic evolution of the Cenozoic Olympic subduction complex, Washington State, as deduced from fission track ages for detrital zircons: *American Journal of Science*, v. 292, p. 565–636.
- Brandon, M.T., Roden-Tice, M.K., and Garver, J.I., 1998, Late Cenozoic exhumation of the Cascadia accretionary wedge in the Olympic Mountains, northwest Washington State: *Geological Society of America Bulletin*, v. 110, p. 985–1009.
- Brozovic, N., Burbank, D., and Meigs, A., 1997, Climatic limits on landscape development in the northwestern Himalaya: *Science*, v. 276, p. 571–574.
- Bucknam, R.C., Hemphill-Haley, E., and Leopold, E.B., 1992, Abrupt uplift within the past 1700 years at southern Puget Sound, Washington: *Science*, v. 258, p. 1611–1614.
- Bull, W.B., 1991, *Geomorphic response to climate change*: Oxford University Press, New York, 326 p.
- Campbell, K.A., and Nesbitt, E.A., 2000, High resolution architecture and paleoecology of an active margin, storm-flood influenced estuary, Quinault Formation (Pliocene), Washington: *Palaios*, v. 15, n. 6, p. 553–579.
- Chappell, J., Omura, A., Esat, T., McCulloch, M., Pandolfi, J., Ota, Y., and Pillans, B., 1996, Reconciliation of late Quaternary sea levels derived from coral terraces at Huon Peninsula with deep sea oxygen isotope records: *Earth and Planetary Science Letters*, v. 141, p. 227–236.
- Cleveland, W.S., 1979, Robust locally weighted regression and smoothing scatterplots: *Journal of the American Statistics Association*, v. 74, p. 829–836.
- Cleveland, W.S., 1981, LOWESS: A program for smoothing scatterplots by robust locally weighted regression: *American Statistician*, v. 35, p. 54.
- Clowes, R.M., Brandon, M.T., Green, A.C., Yorath, C.J., Sutherland Brown, A., Kanasewich, E.R., and Spencer, C., 1987, LITHOPROBE - southern Vancouver Island: Cenozoic subduction complex imaged by deep seismic reflections: *Canadian Journal of Earth Sciences*, v. 24, p. 31–51.
- Crosson, R.S., and Owens, T.J., 1987, Slab geometry of the Cascadia subduction zone beneath Washington from earthquake hypocenters and teleseismic converted waves: *Geophysical Research Letters*, v. 14, p. 824–827.
- Darenzio, M.E., and Peterson, C.D., 1990, Episodic tectonic subsidence of late Holocene salt marshes, northern Oregon coast, central Cascadia margin, U.S.A.: *Tectonics*, v. 9, p. 1–22.
- DeMets, C., and Dixon, T., 1999, New kinematic models for Pacific-North America motion from 3 Ma to present; I, Evidence for steady motion and biases in the NUVEL-1A model: *Geophysical Research Letters*, v. 26, no. 13, p. 1921–1924.
- DeMets, C., Gordon, R.G., Argus, D.F., and Stein, S., 1990, Current plate motions: *Geophysical Journal International*, v. 101, p. 425–478.
- Dethier, D.P., 1986, Weathering rates and the chemical flux from catchments in the Pacific Northwest, U.S.A., in Colman, S., and Dethier, D.P., eds., *Rates of chemical weathering of rocks and minerals*: Academic Press, Orlando, Florida, p. 503–530.
- Dragert, H., 1987, The fall (and rise) of central Vancouver Island: 1930–1985: *Geological Survey of Canada Contribution 10586*, p. 689–697.
- Dragert, H., Hyndman, R.D., Rogers, G.C., and Wang, K., 1994, Current deformation and the width of the seismogenic zone of the northern Cascadia subduction thrust: *Journal of Geophysical Research*, ser. B, v. 99, p. 653–668.
- Durham, J.W., 1944, Megafaunal zones of the Oligocene of northwestern Washington: *University of California Publications in Geological Sciences*, v. 27, p. 101–211.
- Easterbrook, D.J., 1986, Stratigraphy and chronology of Quaternary deposits of the Puget lowland and Olympic Mountains of Washington and the Cascade Mountains of Washington and Oregon, in Sibrava, V., Bowen, D.Q., and Richmond, G.M., eds., *Quaternary glaciations in the Northern Hemisphere*: *Quaternary Science Reviews*, v. 5, p. 145–159.
- Florer, L.E., 1972, Quaternary paleoecology and stratigraphy of the sea cliffs, western Olympic Peninsula, Washington: *Quaternary Research*, v. 2, p. 202–216.
- Garcia, A.F., 1996, Active tectonic deformation and late Pleistocene and Holocene geomorphic and soil profile evolution in the Dosewallips River drainage basin, Olympic Mountains, western Washington State [M.S. thesis]: Albuquerque, The University of New Mexico, 152 p.
- Gerstel, W.J., 1999, Deep-seated landslide inventory of the west-central Olympic Peninsula: Washington Division of Geology and Earth Resources Open File Report 99-2, 36 p.
- Heusser, C.J., 1972, Palynology and phytogeographical significance of a late Pleistocene refugium near Kalaloch, Washington: *Quaternary Research*, v. 2, p. 189–201.
- Heusser, C.J., 1974, Quaternary vegetation, climate, and glaciation of the Hoh River valley, Washington: *Geological Society of America Bulletin*, v. 85, p. 1547–1560.
- Heusser, C.J., 1978, Palynology of the Quaternary deposits of the lower Bogachiel River area, Olympic Peninsula, Washington: *Canadian Journal of Earth Sciences*, v. 15, p. 1568–1578.
- Holdahl, S.R., Martin, D.M., and Stoney, W.M., 1987, Methods for combination of water level and leveling measurements to determine vertical crustal motions, in *Proceedings of Symposium on Height Determination and Recent Crustal Movement in Western Europe*: Bonn, Germany, Dümmler Verlag, p. 373–388.
- Holdahl, S.R., Faucher, F., and Dragert, H., 1989, Contemporary vertical crustal motion in the Pacific northwest, in Cohen, S.C., and Vanicek, P., eds., *Slow deformation and transmission of stress in the Earth*: American Geophysical Union Geophysical Monograph 40, International Union of Geodesy and Geophysics Volume 4, p. 17–29.
- Hyndman, R.D., and Wang, K., 1993, Thermal constraints on the zone of major thrust earthquake failure: The Cascadia subduction zone: *Journal of Geophysical Research*, v. 98, p. 2039–2060.
- Irving, E., and Massey, N.W.D., 1990, Paleomagnetism of ocean layers 2 and 3: Evidence from the Metchosis Complex, Vancouver Island: *Physics of Earth and Planetary Interiors*, v. 64, p. 247–260.
- Kelsey, H.M., 1990, Late Quaternary deformation of marine terraces on the Cascadia subduction zone near Cape Blanco, Oregon: *Tectonics*, v. 9, p. 983–1014.
- Kelsey, H.M., and Bockheim, J.G., 1994, Coastal landscape evolution as a function of eustasy and surface uplift rate, Cascadia margin, southern Oregon: *Geological Society of America Bulletin*, v. 106, p. 840–854.
- Koons, P., 1990, Two-sided orogen; collision and erosion from the sandbox to the Southern Alps, New Zealand: *Geology*, v. 18, p. 679–682.
- McCrorry, P.A., 1996, Tectonic model explaining divergent contraction directions along the Cascadia subduction margin, Washington: *Geology*, v. 24, p. 929–932.
- McCrorry, P.A., 1997, Evidence for Quaternary tectonism along the Washington coast: *Washington Geology*, v. 25, p. 14–19.
- McNeill, L.C., Piper, K., Goldfinger, C., Kulm, L., and Yeats, R., 1997, Listic normal faulting on the Cascadia continental margin: *Journal of Geophysical Research*, ser. B, v. 102, p. 12,123–12,138.
- McNeill, L.C., Goldfinger, C., Kulm, L.D., Yeats, R.S., 2000, Tectonics of the Neogene Cascadia forearc drainage; investigations of a deformed late Miocene unconformity: *Geological Society of America Bulletin*, v. 112, p. 1209–1224.
- Meyer, G.A., Wells, S.G., and Jull, A.J.T., 1995, Fire and alluvial chronology in Yellowstone National Park: Climate and intrinsic controls on Holocene geomorphic processes: *Geological Society of America Bulletin*, v. 107, p. 1211–1230.
- Mitchell, C.E., Vincent, P., Weldon R.J., and Richards, M., 1994, Present-day vertical deformation of the Cascadia margin, Pacific Northwest, U.S.A.: *Journal of Geophysical Research*, ser. B, v. 99, p. 12,257–12,277.
- Montgomery, D.R., 2001, Slope distributions, threshold hillslopes, and steady-state topography: *American Journal of Science*, v. 301, p. 432–454.
- Montgomery, D.R., 2002, Valley formation by fluvial and glacial erosion: *Geology*, v. 30, p. 1047–1050.
- Montgomery, D.R., and Greenberg, H., 2000, Local relief and the height of Mount Olympus: *Earth Surface Processes and Landforms*, v. 25, p. 385–396.
- Montgomery, D.R., and Brandon, M.T., 2002, Topographic controls on erosion rates in tectonically active mountain ranges: *Earth and Planetary Science Letters*, v. 201, p. 481–489.
- Muller, J.E., Snavely, P.D., and Tabor, R.W., 1983, The Tertiary Olympic terrane, southwest Vancouver Island and northwest Washington: *Geological Association of Canada, 1983 Annual Meeting, Guidebook for fieldtrip n. 12*, 59 p.
- Niem, W.A., Niem, A.R., and Snavely, P.D., Jr., 1992, Western Washington-Oregon coastal sequence, in Christiansen, R.L., and Yeats, R.S., eds., *Post-Laramide geology of the U.S. Cordilleran region, The Geology of North America*, v. G-3, The Cordilleran Orogen: Conterminous United States: Boulder, Colorado, Geological Society of America, p. 265–270.

- Orange, D.L., 1990, Criteria helpful in recognizing shear-zone and diapiric melanges: Examples from the Hoh accretionary complex, Olympic Peninsula, Washington: *Geological Society of America Bulletin*, v. 102, p. 935–951.
- Palmer, S.P., and Lingley, W.S., Jr., 1989, An assessment of the oil and gas potential of the Washington outer continental shelf: University of Washington, Washington Sea Grant Program, p. 83.
- Pazzaglia, F.J., and Brandon, M.T., 2001, A fluvial record of rock uplift and shortening across the Cascadia forearc high: *American Journal of Science*, v. 301, p. 385–431.
- Pillans, B., Chappell, J., and Naish, T.R., 1998, A review of the Milankovitch climatic beat: Template for Plio-Pleistocene sea-level changes and sequence stratigraphy: *Sedimentary Geology*, v. 122, p. 5–21.
- Prothero, D.R., and Armentrout, J.M., 1985, Magnetostratigraphic correlation of the Lincoln Creek Formation, Washington: Implications for the age of the Eocene-Oligocene boundary: *Geology*, v. 13, p. 208–211.
- Prothero, D.R., and Burns, C., 2001, Magnetic stratigraphy and tectonic rotation of the upper Oligocene-lower Miocene (type Pillarian stage) Clallam Formation, Clallam County, Washington: *Pacific Section Society for Sedimentary Geology Special Publication 91*, p. 234–241.
- Prothero, D.R., Streig, A., and Burns, C., 2001, Magnetic stratigraphy and tectonic rotation of the upper Oligocene Pysht Formation, Clallam County, Washington: *Pacific Section Society for Sedimentary Geology Special Publication 91*, p. 224–233.
- Ramsay, B., 2000, OxCal v. 3.5: available from <http://www.rlaha.ox.ac.uk/orau/index.htm>.
- Rau, W., 1973, Geology of the Washington coast between Point Grenville and the Hoh River: Washington Department of Natural Resources, Geology and Earth Resources Division Bulletin, v. 66, 58 p.
- Rau, W., 1975, Geologic map of the Destruction Island and Taholah quadrangles, Washington: Washington Department of Natural Resources, Geology and Earth Resources Division Map GM-13, scale 1:62,500.
- Rau, W., 1979, Geologic map in the vicinity of the lower Bogachiel and Hoh River valleys and the Washington coast: Department of Natural Resources, Geology and Earth Resources Division Map GM-24, scale 1:62,500.
- Rau, W.W., 1970, Foraminifera, stratigraphy, and paleoecology of the Quinault Formation, Point Grenville-Raft River coastal area, Washington: Washington Department of Natural Resources Bulletin, v. 62, 34 p.
- Rau, W.W., and Grocock, G., 1974, Piercement structure outcrops along the Washington coast: Washington, Department of Natural Resources, Division of Mines and Geology, Information Circular, v. 51, 7 p.
- Reilinger, R., and Adams, J., 1982, Geodetic evidence for active landward tilting of the Oregon and Washington Coastal Ranges: *Geophysical Research Letters*, v. 9, p. 401–403.
- Roering, J.J., Kirchner, J.W., Sklar, L.S., Dietrich, W.E., 2001, Hillslope evolution by nonlinear creep and landsliding: An experimental study: *Geology*, v. 29, p. 143–146.
- Rogers, G.C., 1988, An assessment of megathrust earthquake potential of the Cascadia subduction zone: *Canadian Journal of Earth Science*, v. 25, p. 844–852.
- Savage, J.C., Lisowski, M., and Prescott, W.H., 1981, Geodetic strain measurements in Washington: *Journal of Geophysical Research*, ser. B, v. 86, p. 4929–4940.
- Savage, J.C., Lisowski, M., and Prescott, W.H., 1991, Strain accumulation in western Washington: *Journal of Geophysical Research*, ser. B, v. 96, p. 14,493–14,507.
- Serdar, C.F., 1999, Description, analysis and impacts of the Grouse Creek landslide, Jefferson County, Washington, 1997–98: The Evergreen State College Master of Environmental Studies thesis, 171 p.
- Snively, P.D., Jr., Niem, A.R., and Pearl, J.E., 1978, Twin River Group (upper Eocene to lower Miocene) defined to include Hoko River, Makah, and Pysht Formations, Clallam County, Washington: U.S. Geological Survey Bulletin, v. 1457A, p. A111–A120.
- Stewart, R.J., and Brandon, M.T., 2003, Detrital zircon fission-track ages for the “Hoh Formation”: Implications for late Cenozoic evolution of the Cascadia subduction wedge: *Geological Society of America Bulletin* (in press).
- Symons, D.T.A., 1973, Paleomagnetic zones in the Oligocene East Sooke Gabbro, Vancouver Island, British Columbia: *Journal of Geophysical Research*, v. 78, p. 5100–5109.
- Tabor, R., 1975, Guide to the geology of Olympic National Park: Seattle, University of Washington Press, 144 p.
- Tabor, R., and Cady, W., 1978b, The structure of the Olympic Mountains, Washington—Analysis of a subduction zone: U.S. Geological Survey Professional Paper 1033, 38 p.
- Tabor, R.W., and Cady, W.M., 1978a, Geologic map of the Olympic Peninsula: U.S. Geological Survey Map I-994, 2 sheets, scale 1:125,000.
- Thackray, G.D., and Pazzaglia, F.J., 1994, Quaternary stratigraphy, tectonic geomorphology, and fluvial evolution of the western Olympic Peninsula, Washington, in Swanson, D.A., and Haugerud, R.A., eds., *Geologic field trips in the Pacific Northwest, 1994 Geological Society of America Annual Meeting*, Seattle, Washington, p. 2A-1–2A-30.
- Thackray, G.D., 1996, Glaciation and neotectonic deformation on the western Olympic Peninsula, Washington [Ph.D. dissertation]: Seattle, Washington, University of Washington, 139 p.
- Thackray, G.D., 1998, Convergent-margin deformation of Pleistocene strata on the Olympic coast of Washington, USA, in Stewart, I.S., and Vita-Finzi, C., eds., *Coastal tectonics: Geological Society [London] Special Publication 146*, p. 199–211.
- Thackray, G.D., 2001, Extensive Early and Middle Wisconsin glaciation on the western Olympic Peninsula, Washington, and the variability of Pacific moisture delivery to the northwestern United States: *Quaternary Research*, v. 55, p. 257–270.
- Thatcher, W., and Rundle, J.B., 1984, A viscoelastic coupling model for the cyclic deformation due to periodically repeated earthquakes at subduction zones: *Journal of Geophysical Research*, ser. B, v. 89, p. 7631–7640.
- Thorson, R.M., 1989, Glacio-isostatic response of the Puget Sound area, Washington: *Geological Society of America Bulletin*, v. 101, p. 1163–1174.
- Tomkin, J.H., Brandon, M.T., Pazzaglia, F.J., Barbour, J.R., and Willett, S.D., 2003, Quantitative testing of bedrock incision models, Clearwater River, WA: *Journal of Geophysical Research* (in press).
- Wang, K., 1996, Simplified analysis of horizontal stresses in a buttressed forearc sliver at an oblique subduction zone: *Geophysical Research Letters*, v. 23, p. 2021–2024.
- Wegmann, K., 1999, Late Quaternary fluvial and tectonic evolution of the Clearwater River basin, western Olympic Mountains, Washington State [M.S. thesis]: Albuquerque, University of New Mexico, 217 p., 4 plates.
- Wegmann, K., and Pazzaglia, F.J., 2002, Holocene strath terraces, climate change, and active tectonics: the Clearwater River basin, Olympic Peninsula, Washington State: *Geological Society of America Bulletin*, v. 114, no. 6, p. 731–744.
- Wells, R., Weaver, C., and Blakely, R., 1998, Fore-arc migration in Cascadia and its neotectonic significance: *Geology*, v. 26, p. 759–762.
- Wells, R.E., 1990, Paleomagnetic rotations and the Cenozoic tectonics of the Cascade Arc, Washington, Oregon, and California: *Journal of Geophysical Research*, v. 95, p. 19,409–19,417.
- Wells, R.E., and Coe, R.S., 1985, Paleomagnetism and geology of Eocene volcanic rocks of southwest Washington: Implications for mechanisms of tectonic rotation: *Journal of Geophysical Research*, v. 90, p. 1925–1947.
- West, D.O., and McCrumb, D.R., 1988, Coastline uplift in Oregon and Washington and the nature of Cascadia subduction zone tectonics: *Geology*, v. 16, p. 169–172.
- Willett, S., 1999, Orogeny and orography: The effects of erosion on the structure of mountain belts: *Journal of Geophysical Research*, v. 104, p. 28,957–28,981.
- Willett, S.D., and Brandon, M.T., 2002, On steady states in mountain belts: *Geology*, v. 30, p. 175–178.
- Willett, S., Beaumont, C., and Fullsack, P., 1993, Mechanical models for the tectonics of doubly vergent compressional orogens: *Geology*, v. 21, p. 371–374.
- Willett, S.D., Slingerland, R., and Hovius, N., 2001, Uplift, shortening, and steady state topography in active mountain belts: *American Journal of Science*, v. 301, p. 455–485.

